

2

NAVAL POSTGRADUATE SCHOOL

Monterey, California

AD-A242 976



DTIC
ELECTE
DEC 5 1991
S C D



THESIS

A DISCONTINUITY STUDY IN SHIELDED
COPLANAR LINE

by

Hwang, J. S.

December 1990

Thesis Advisor

H.A. Atwater

Approved for public release; distribution is unlimited.

91-17043



91 12 0 39

Unclassified

security classification of this page

REPORT DOCUMENTATION PAGE

1a Report Security Classification Unclassified		1b Restrictive Markings	
2a Security Classification Authority		3 Distribution/Availability of Report	
2b Declassification/Downgrading Schedule		Approved for public release; distribution is unlimited.	
4 Performing Organization Report Number(s)		5 Monitoring Organization Report Number(s)	
6a Name of Performing Organization Naval Postgraduate School	6b Office Symbol (if applicable) 3A	7a Name of Monitoring Organization Naval Postgraduate School	
6c Address (city, state, and ZIP code) Monterey, CA 93943-5000		7b Address (city, state, and ZIP code) Monterey, CA 93943-5000	
8a Name of Funding Sponsoring Organization	8b Office Symbol (if applicable)	9 Procurement Instrument Identification Number	
8c Address (city, state, and ZIP code)		10 Source of Funding Numbers	
		Program Element No	Project No
		Task No	Work Unit Accession No
11 Title (include security classification) A DISCONTINUITY STUDY IN SHIELDED COPLANAR LINE			
12 Personal Author(s) Hwang, J. S.			
13a Type of Report Master's Thesis	13b Time Covered From To	14 Date of Report (year, month, day) December 1990	15 Page Count 70
16 Supplementary Notation The views expressed in this thesis are those of the author and do not reflect the official policy or position of the Department of Defense or the U.S. Government.			
17 Cosatl Codes		18 Subject Terms (continue on reverse if necessary and identify by block number)	
Field	Group	Subgroup	
		A discontinuity study in shielded coplanar line	
19 Abstract (continue on reverse if necessary and identify by block number)			
<p>A study of the shielded coplanar line (SCPL) is presented. The main goal of this thesis is to develop an equivalent circuit model for a typical discontinuity in the SCPL. The formulation is based on Galerkin's method, using Green's function applied in the Fourier transform domain.</p> <p>The impedance (Z_o) has been calculated by using a variational method. The propagation constant ($\beta(\omega)$) and effective dielectric constant (ϵ_{reff}) of the SCPL have been calculated by using the method of moments. The cut-off frequency of this waveguide has been obtained by a theorem of Van Bladel and Higgins.</p>			
20 Distribution/Availability of Abstract		21 Abstract Security Classification	
<input checked="" type="checkbox"/> unclassified/unlimited users <input type="checkbox"/> same as report <input type="checkbox"/> DTIC		Unclassified	
22a Name of Responsible Individual H.A. Atwater		22b Telephone (include Area code) 408-646-3001	22c Office Symbol EC/AN

Approved for public release; distribution is unlimited.

A Discontinuity Study in Shielded Coplanar Line

by

Hwang, J. S.
LCDR , Korean Navy
B.S., Naval Academy Korea , 1980

Submitted in partial fulfillment of the
requirements for the degree of

MASTER OF SCIENCE IN ELECTRICAL AND COMPUTER ENGINEERING

from the

NAVAL POSTGRADUATE SCHOOL
December 1990

Author:

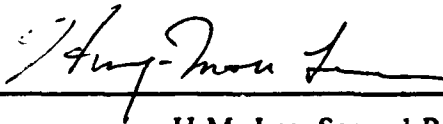


Hwang, J. S.

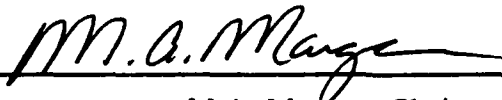
Approved by:



H.A. Atwater, Thesis Advisor



H.M. Lee, Second Reader



M.A. Morgan, Chairman,
Department of Electrical and Computer Engineering

ABSTRACT

A study of the shielded coplanar line (SCPL) is presented. The main goal of this thesis is to develop an equivalent circuit model for a typical discontinuity in the SCPL. The formulation is based on Galerkin's method, using Green's function applied in the Fourier transform domain.

The impedance (Z_0) has been calculated by using a variational method. The propagation constant ($\beta(\omega)$) and effective dielectric constant (ϵ_{reff}) of the SCPL have been calculated by using the method of moments. The cut-off frequency of this waveguide has been obtained by a theorem of Van Bladel and Higgins.

Accession For	
NTIS GRA&I	<input checked="" type="checkbox"/>
DTIC TAB	<input type="checkbox"/>
Unannounced	<input type="checkbox"/>
Justification	
By _____	
Distribution/	
Availability Codes	
Dist	Avail and/or Special
A-1	

TABLE OF CONTENTS

I. INTRODUCTION	1
II. THEORETICAL ANALYSIS	3
A. FOURIER-TRANSFORMED GALERKIN'S METHOD FOR THE SCPL RESONATOR	4
B. GREEN'S FUNCTION FOR THE MOMENT METHOD .	10
C. CUT-OFF FREQUENCY IN TWO-DIELECTRIC LAY- ERED RECTANGULAR WAVEGUIDES	12
III. COMPUTER PROGRAM CONSTRUCTION	20
A. CURRENT DISTRIBUTIONS	20
B. COMPUTATION PROCEDURE	23
1. Change of Transform Variable	23
C. CALCULATION OF FRINGING CAPACITANCE	25
1. HALF-WAVELENGTH RESONATOR ASSUMPTION	26
2. TERMINATED TRANSMISSION-LINE MODEL ...	27
IV. RESULT OF COMPUTATION	30
A. SCPL WITH VARYING DIELECTRIC CONSTANT	30
B. SCPL WITH VARYING CONDUCTOR SPACING	34
C. SCPL WITH VARYING WIDTH OF THE CENTER CON- DUCTOR	37
D. SCPL WITH VARYING HEIGHT OF DIELECTRIC LAYER.	40

V. CONCLUSION	43
APPENDIX A. FORTRAN PROGRAMS	44
A. RESONANT FREQUENCY	44
B. THE FRINGING CAPACITANCE	50
C. PROPAGATION CONSTANT	51
D. CUT - OFF FREQUENCY	53
APPENDIX B. IMPEDANCE AND DIELECTRIC CONSTANT BY VARIATIONAL METHOD	54
LIST OF REFERENCES	57
INITIAL DISTRIBUTION LIST	58

LIST OF TABLES

Table 1.	CONFIGURATION DATA IN SCPL	19
Table 2.	VARIATION OF NUMBER OF TERMS N	24
Table 3.	VARIATION OF NUMBER OF TERMS M	25
Table 4.	CONFIGURATION DATA IN SCPL	31
Table 5.	CONFIGURATION DATA IN SCPL	34
Table 6.	CONFIGURATION DATA IN SCPL	37
Table 7.	CONFIGURATION DATA IN SCPL	40

LIST OF FIGURES

Figure 1. Top and End view of SCPL	3
Figure 2. Cross sections of the waveguide	12
Figure 3. Form of assumed current distributions	20
Figure 4. Terminated transmission line model	28
Figure 5. Magnitude and Phase of Z_{in} for terminated line-segment	29
Figure 6. Cross section view of SCPL	30
Figure 7. ΔC and f_o versus ϵ_r in SCPL	32
Figure 8. Z_o and ϵ_{reff} versus ϵ_r in SCPL	33
Figure 9. ΔC and f_o versus GAP/D in SCPL	35
Figure 10. Z_o and ϵ_{reff} versus GAP/D in SCPL	36
Figure 11. ΔC and f_o versus A/D in SCPL	38
Figure 12. Z_o and ϵ_{reff} versus A/D in SCPL	39
Figure 13. ΔC and f_o versus D in SCPL	41
Figure 14. Z_o and ϵ_{reff} versus D in SCPL	42

Figure 15. Assumed line-charge density function of SCPL 54

ACKNOWLEDGEMENTS

I would like to thank the Korean Navy for the opportunity to study at the Naval Postgraduate School. I wish to thank to Dr. H.A. Atwater for his patient guidance, continuous assistance and very helpful criticism throughout this work. I am very grateful to Dr. H.M. Lee whose comments and recommendations contributed to the successful completion of this thesis. Finally, I am also grateful to my wife, Yong Hee and daughters, Sang Mi, Sang Yae, for their support and patience.

I. INTRODUCTION

The shielded coplanar line (SCPL) is useful for radar and communication circuits at microwave and millimeter-wave frequencies. In order to use this transmission medium in the construction of microwave circuits and filters, it is necessary to have valid circuit models for typical discontinuities such as the series gap in line, open-ended stub, and a discontinuous change in width. There is a definite need for an accurate full-wave analysis of strip transmission line structures. By full wave analysis is implied the process of rigorously solving the frequency dependent electromagnetic (EM) boundary value problem with retention of all the field components. In this thesis, the boundary value problem associated with the discontinuity structure of interest incorporated in a SCPL resonator has been solved in a formulation employing full-wave analysis. The solution of the problem has been derived using an efficient method. Specifically, the derivation of the characteristic equation for resonant frequencies of a resonator model is carried out using Galerkin's technique applied in the spectral or Fourier transform domain instead of the space domain. The resonant frequency of the structure of interest is obtained

by numerically solving the characteristic equation. The details of the analysis method will appear in Chapter II of this work.

In Chapter III, at the discontinuity in an open-ended resonator, the fringing capacitance of the open end will be calculated by two methods.

II. THEORETICAL ANALYSIS

The shielded coplanar line (SCPL) to be analyzed is shown in Fig.1. A strip conductor is located symmetrically between ground strips on both sides. The strips are placed on the dielectric substrate. The SCPL is constructed by placing dielectric and conductor within a closed channel forming a shield. Dimensions must be sufficiently small to avoid propagation of waveguide modes within the channel.

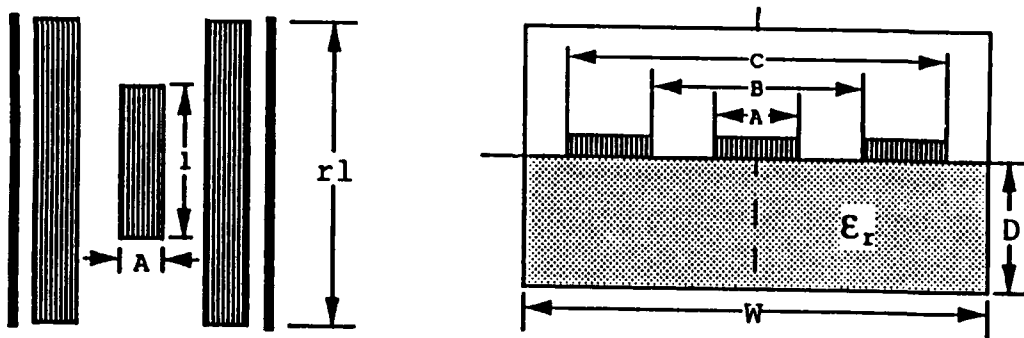


Figure 1. Top and End view of SCPL

It is assumed that the thickness of the conducting strip is negligible and that all the media and conductors are lossless. For simplicity, the

center and the ground strip are to be located symmetrically in the z-direction within the ends of the shielding enclosure.

A. FOURIER-TRANSFORMED GALERKIN'S METHOD FOR THE SCPL RESONATOR

The analysis of wave propagation on the SCPL systems of the type considered here has been carried out by Itoh and Uwano [Ref.2]. These authors treated the problem using Galerkin's method of moments in the Fourier-Transform domain. Their work is summarized in terms of a set of Green's function equations:

$$\tilde{Z}_{zz}\tilde{J}_z + \tilde{Z}_{zx}\tilde{J}_x = \tilde{E}_z \quad (1a)$$

$$\tilde{Z}_{xz}\tilde{J}_z + \tilde{Z}_{xx}\tilde{J}_x = \tilde{E}_x \quad (1b)$$

Where $\tilde{J}_z = \tilde{J}_z(k_n, \beta_m)$, $\tilde{J}_x = \tilde{J}_x(k_n, \beta_m)$.

In Eqs.(1a) and (1b), J_z and J_x are the z and x components of the currents on the strip conductor, and E_z and E_x are the components of electric field tangent to the substrate surface, and the \tilde{Z}_y are Green's functions.

The tildes over the factors in Eqs.(1a) and (1b) imply Fourier transformation of the respective quantities. In this work, the Fourier trans-

formation is carried out in the bounded region interior to the shielding enclosure placed around the line segment representing the resonator.

There we have the finite Fourier transformation:

$$\tilde{f}(k_n, \beta_m) = \int_{-rl/2}^{+rl/2} dz \int_{-a/2}^{+a/2} f(x,z) \exp(jk_n x) \exp(j\beta_m z) dx \quad (2)$$

where k_n, β_m are the discrete transform variables defined by,

$$k_n = (n - 1/2)\pi/a \quad \text{for } E_z \text{ even, } -H_z \text{ odd (in } x \text{) modes}$$

$$k_n = n\pi/a \quad \text{for } E_z \text{ odd, } -H_z \text{ even (in } x \text{) modes}$$

$$\beta_m = (m - 1/2)\pi/rl \quad \text{for } E_z \text{ even, } -H_z \text{ odd (in } z \text{) modes}$$

where a is the width of the waveguide enclosure, and rl is its length.

The analytical task then consists of assuming suitable coordinate forms for the current densities J_z and J_x , and Fourier-transforming these. Inner products are then formed in Eqs.(1a) and (1b), in accordance with the standard procedure of the method moments. This procedure gives rise to a set of homogeneous equations in the unknown coefficients assumed in J_z and J_x . The solution condition for the simultaneous equations leads to a determination of the resonance frequency of the SCPL resonator of the problem. The unknowns E_z and E_x can be eliminated by applying Galerkin's method in the spectral domain. The first

step is to expand the unknown J_z and J_x in terms of assumed basis functions J_{zi} and J_{xj} with unknown coefficients c_j and d_i .

$$\tilde{J}_z = \sum_{i=1}^{N1} d_i \tilde{J}_{zi}(k_n, \beta_m) \quad (3a)$$

$$\tilde{J}_x = \sum_{j=1}^{N2} c_j \tilde{J}_{xj}(k_n, \beta_m) \quad (3b)$$

The basis functions \tilde{J}_{zi} and \tilde{J}_{xj} must be chosen to be the Fourier transforms of space-domain functions $J_{zi}(x,z)$ and $J_{xj}(x,z)$ which are physically realistic, and which are zero except for the region $|x| < A/2$ and $|z| < l/2$. Substituting (3) into (1) yields the matrix equations,

$$\tilde{Z}_{zz} \sum_{i=1}^{N1} d_i \tilde{J}_{zi} + \tilde{Z}_{zx} \sum_{j=1}^{N2} c_j \tilde{J}_{xj} = \tilde{E}_z \quad (4a)$$

$$\tilde{Z}_{xz} \sum_{i=1}^{N1} d_i \tilde{J}_{zi} + \tilde{Z}_{xx} \sum_{j=1}^{N2} c_j \tilde{J}_{xj} = \tilde{E}_x \quad (4b)$$

Where $\tilde{J}_{zi} = \tilde{J}_{zi}(k_n, \beta_m)$, $\tilde{J}_{xj} = \tilde{J}_{xj}(k_n, \beta_m)$. Taking products of the resulting Eqs.(4a) and (4b) with the basis functions and for different values of i, j, yields the matrix equations:

$$\tilde{J}_{zk} \tilde{Z}_{zz} \sum_{i=1}^{N1} d_i \tilde{J}_{zi} + \tilde{J}_{zk} \tilde{Z}_{zx} \sum_{j=1}^{N2} c_j \tilde{J}_{xj} = \tilde{J}_{zk} \tilde{E}_z \quad (4c)$$

$$\tilde{J}_{xl} \tilde{Z}_{xz} \sum_{i=1}^{N1} d_i \tilde{J}_{zi} + \tilde{J}_{xl} \tilde{Z}_{xx} \sum_{j=1}^{N2} c_j \tilde{J}_{xj} = \tilde{J}_{xl} \tilde{E}_x \quad (4d)$$

Making summations of Eqs.(4c) and (4d) to complete the inner products, yields the matrix equations:

$$\sum_{m=-\infty}^{+\infty} \sum_{n=-\infty}^{+\infty} \tilde{J}_{zk} \tilde{Z}_{zz} \sum_{i=1}^{N1} d_i \tilde{J}_{zi} + \sum_{m=-\infty}^{+\infty} \sum_{n=-\infty}^{+\infty} \tilde{J}_{zk} \tilde{Z}_{zx} \sum_{j=1}^{N2} c_j \tilde{J}_{xj} = \sum_m \sum_n \tilde{J}_{zk} \tilde{E}_z \quad (5a)$$

$$\begin{aligned}
& \sum_{m=-\infty}^{+\infty} \sum_{n=-\infty}^{+\infty} \tilde{J}_{xl} \tilde{Z}_{zx} \sum_{i=1}^{N1} d_i \tilde{J}_{zi} \\
& + \sum_{m=-\infty}^{+\infty} \sum_{n=-\infty}^{+\infty} \tilde{J}_{xl} \tilde{Z}_{xx} \sum_{j=1}^{N2} c_j \tilde{J}_{xj} = \sum_m \sum_n \tilde{J}_{xl} \tilde{E}_x
\end{aligned} \tag{5b}$$

The right-hand sides of Eqs (5a). and (5b) are zero by virtue of Parseval's theorem, because the currents $J_{zi}(x)$, $J_{xj}(x)$ and the field components $E_z(x,d)$, $E_x(x,d)$ vanish in complementary regions of x . For example, when the inner product of $\tilde{J}_{zk} \tilde{E}_z$ on the right-hand side of Eqs.(5a) and (5b) is taken, $J_{zk}(x)$ is zero outside the strip, and $E_z(x)$ is zero on the strip. Therefore, the final boundary condition is satisfied. Equations (5a) and (5b) will be expressed in matrix form as follows:

$$\sum_{i=1}^{N1} d_i K_{ki}^{(1,1)} + \sum_{j=1}^{N2} c_j K_{ki}^{(1,2)} = 0 \tag{5c}$$

$$\sum_{i=1}^{N1} d_i K_{li}^{(2,1)} + \sum_{j=1}^{N2} c_j K_{lj}^{(2,2)} = 0 \quad (5d)$$

Where

$$K_{ki}^{(1,1)}(\omega_o) = \sum_{m=-\infty}^{+\infty} \sum_{m=-\infty}^{+\infty} \tilde{J}_{zk}(k_n, \beta_m) \tilde{Z}_{zz} \tilde{J}_{zi}(k_n, \beta_m) \quad (6a)$$

$$K_{kj}^{(1,2)}(\omega_o) = \sum_{m=-\infty}^{+\infty} \sum_{m=-\infty}^{+\infty} \tilde{J}_{zk}(k_n, \beta_m) \tilde{Z}_{zx} \tilde{J}_{xj}(k_n, \beta_m) \quad (6b)$$

$$K_{li}^{(2,1)}(\omega_o) = \sum_{m=-\infty}^{+\infty} \sum_{m=-\infty}^{+\infty} \tilde{J}_{xl}(k_n, \beta_m) \tilde{Z}_{xz} \tilde{J}_{zi}(k_n, \beta_m) \quad (6c)$$

$$K_{lj}^{(2,2)}(\omega_o) = \sum_{m=-\infty}^{+\infty} \sum_{m=-\infty}^{+\infty} \tilde{J}_{xl}(k_n, \beta_m) \tilde{Z}_{xx} \tilde{J}_{xj}(k_n, \beta_m) \quad (6d)$$

Where $\tilde{Z}_{pq} = \tilde{Z}_{pq}(k_n, \beta_m)$.

A homogeneous system of equations is thus obtained in terms of the unknown coefficients c_j , d_i . In order that c_j and d_i have nontrivial solutions, the determinant of the matrix must be zero, and hence the resonant frequency is determined for the resonator.

Equations (5) are now solved for the angular frequency ω_0 by seeking the root of the resulting characteristic equation. The resonance frequency of the SCPL strip line resonator is derived from the obtained value of ω_0 . The accuracy of the solution can be systematically improved by increasing the number of basis functions (N_1, N_2) and by solving larger size matrix equations. However, if the first few basis function are chosen so as to approximate the actual unknown current distribution reasonably well, the necessary size of the matrix can be held small for a given accuracy of the solution, resulting in numerical efficiency. Hence the choice of basis functions is important from the numerical point of view.

B. GREEN'S FUNCTION FOR THE MOMENT METHOD

Equations (1a) and (1b) may be expressed in the matrix form [Ref.2]:

$$\begin{bmatrix} \tilde{E}_z \\ \tilde{E}_x \end{bmatrix} = \begin{bmatrix} \tilde{Z}_{zz} & \tilde{Z}_{zx} \\ \tilde{Z}_{xz} & \tilde{Z}_{xx} \end{bmatrix} \begin{bmatrix} \tilde{J}_z \\ \tilde{J}_x \end{bmatrix} \quad (7)$$

where the transformed Green's functions have the values:

$$\tilde{Z}_{xz} = k_n \beta \frac{(RTH2 + RTH1)}{ZED} \quad (8a)$$

$$\tilde{Z}_{zz} = \frac{[(k_n^2 - \gamma_1^2)RTH2 + (k_n^2 - \gamma_2^2)RTH1]}{ZED} \quad (8b)$$

$$\tilde{Z}_{xx} = (k_n^2 - \gamma_1^2)RTH1 \frac{1}{ZED} \quad (8c)$$

$$\tilde{Z}_{zx} = \tilde{Z}_{xz}$$

$$ZED = (RTH1 + ER \times RTH2) \left(\frac{\gamma_1^2}{RTH1} + \frac{\gamma_2^2}{RTH2} \right)$$

Case1 $\gamma_i^2 \geq 0$

$$RTH1 = \gamma_1 \tanh(\gamma_1 d)$$

$$RTH2 = \gamma_2 \tanh(\gamma_2 h)$$

case2 $\gamma_i^2 < 0$

$$RTH1 = -\gamma_1 \tan(\gamma_1 h)$$

$$RTH2 = -\gamma_2 \tan(\gamma_2 h)$$

$$\gamma_i = \sqrt{k_n^2 + \beta_m^2 - \mu_o \epsilon_i \omega^2}$$

Where $i = 1, 2$ in the indicated layer. The quantities $\tilde{Z}_{zz}, \tilde{Z}_{zx}, \tilde{Z}_{xx}$ are actually the Fourier transforms of dyadic Green's function components.

C. CUT-OFF FREQUENCY IN TWO-DIELECTRIC LAYERED RECTANGULAR WAVEGUIDES

If a rectangular wave guide is partially filled with a solid dielectric arranged as indicated in Fig.1, this dielectric results in lowering the cut-off frequency and phase velocities of the modes as compared with that of a guide of the same dimensions wholly filled with air.

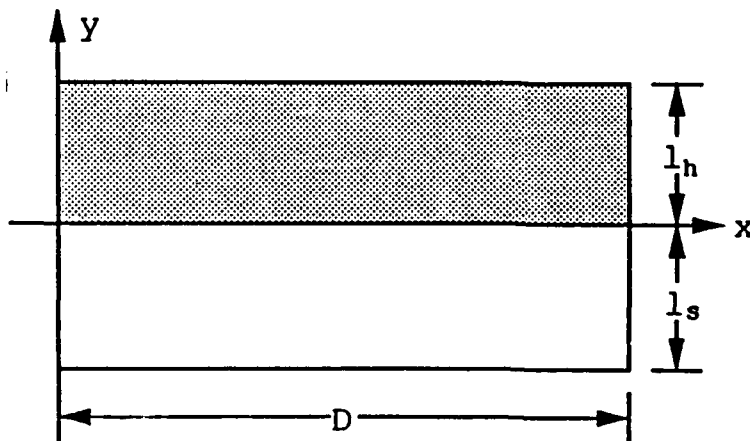


Figure 2. Cross sections of the waveguide

These effects have led to several important technical uses of layered-dielectric guides. The field in the guide is a linear combination of elemental waves, infinite in number, and termed normal modes. These modes are to be found by taking a z (axial) dependence of the form $\exp(jhz)$ for the six components of \tilde{E} and \tilde{H} and by constructing, through separation of variables, a wave which matches all boundary conditions. This procedure, as is illustrated below, yields a relation between h^2 and ω^2 termed the characteristic equation of such form that, for a given angular frequency ω , h^2 can take only a discrete, though infinite, set of values (the eigenvalues). To each eigenvalue corresponds a mode. When the eigenvalue h^2 is negative, h is imaginary, $\exp(jhz)$ is a damping factor and the mode is not propagated. When h^2 is positive, the mode is propagated. The transition between these two states occurs at a frequency termed the cut-off frequency of the mode, for which h^2 is equal to zero. The lowest of these modal cut-off frequencies is the fundamental cut-off frequency of the guide, below which no energy can be propagated in the guide. It follows from Maxwell's equations that the field components of

a mode can be expressed as a function of E_z and H_z , by the equations [Ref.11]:

$$\left(\frac{\omega^2}{c^2}\right)\bar{E}_c = k^2\bar{E}_c = jh(\nabla E_z) + j\omega\mu(\bar{k}_x\nabla H_z) \quad (9a)$$

$$\left(\left(\frac{\omega^2}{c^2}\right) - h^2\right)\bar{H}_c = k^2\bar{H}_c = jh(\nabla H_z) - j\omega\varepsilon(\bar{k}_x\nabla E_z) \quad (9b)$$

where the subscript c denotes a component in the plane of the cross section, \bar{k} is a unit-vector directed along the z-axis, and $\bar{E}_c, \bar{E}_z, \bar{H}_c, \bar{H}_z$ determine the (x,y) dependent part of a component. Thus, typically

$$E_z = \bar{E}_z(x, y) \exp(j(\omega t + hz))$$

It also follows from Maxwell's equations that in each homogeneous medium, E_z and H_z satisfy Helmholtz's equation.

$$\nabla_{xy}^2 A + k^2 A = 0, \quad A = (E_z, H_z)$$

Equations (9) and (10) enable expression of the boundary conditions on E_z and H_z . The conditions at a metallic wall are $E_z = \frac{\partial H_z}{\partial n} = 0$; the

conditions at a dielectric interface, in the particular case of Fig.2, are that the quantities:

$$\frac{jh}{k_i^2} \frac{\partial}{\partial x} E_z - \frac{j\omega\mu_i}{k_i^2} \frac{\partial}{\partial y} H_z \quad (10a)$$

and,

$$\frac{jh}{k_i^2} \frac{\partial}{\partial x} H_z + \frac{j\omega\varepsilon_i}{k_i^2} \frac{\partial}{\partial y} E_z, \quad (i = h, s) \quad (10b)$$

be continuous at the interface. These considerations are applied to the guide depicted in Fig.2. Separation of variables in Eqs.(9a), (9b) and application of boundary conditions at the metallic walls yields

$$E_{zh} = A_h \sin(m\pi \frac{x}{d}) \sin(u_h \frac{(y - l_h)}{l_h}) \quad (11a)$$

$$E_{zs} = A_h \cos(m\pi \frac{x}{d}) \cos(u_s \frac{(y - l_s)}{l_s}) \quad (11b)$$

$$H_{zh} = B_h \cos(m\pi \frac{x}{d}) \cos(u_h \frac{(y - l_h)}{l_h}) \quad (11c)$$

$$H_{zs} = B_s \cos(m\pi \frac{x}{d}) \cos(u_h \frac{(y - l_s)}{l_s}) \quad (11d)$$

Where subscript h refers to the dielectric, and s to the air media, and m is integer (including zero). Let U_i be an auxiliary variable defined by

$$U_i = ((\frac{\omega^2}{c_i^2}) - h^2 - (\frac{m\pi}{d})^2 l_i)^{1/2}, \quad i = h, s \quad (12)$$

Applying the boundary conditions at the dielectric interface through substituting Eqs.(11) in Eqs.(9) and (10) and setting $y = 0$ yields:

$$A_h \sin(U_h) + A_s \sin(U_s) = 0 \quad (13a)$$

$$B_h \cos(U_h) - B_s \cos(U_s) = 0 \quad (13b)$$

$$A_h \frac{hm\pi}{d} \frac{\sin(U_h)}{kh^2} + A_s \frac{hm\pi}{d} \sin \frac{(U_s)}{k_s^2} + B_h \frac{\omega U_h}{k_h^2} U_h \sin \frac{(U_h)}{l_h} + B_s \frac{\omega U_s}{k_s^2} U_s \frac{\sin(U_s)}{l_s} = 0 \quad (13c)$$

$$\begin{aligned}
& A_h \frac{\omega \varepsilon_h}{k_h^2} \frac{U_h \cos U_h}{l_h} - A_s \frac{\omega \varepsilon_s}{k_s^2} \frac{U_s \cos U_s}{l_s} - B_h \frac{hm\pi}{d} \frac{\cos U_h}{k_h^2} \\
& + B_s \frac{hm\pi}{d} \frac{\cos U_s}{k_s^2} = 0
\end{aligned} \tag{13d}$$

The determinant of the coefficients of this system of four homogeneous linear equations in A_h, A_s, B_h, B_s , must be zero in order that the field be nonvanishing. Formulating this condition yields the characteristic equation,

$$\begin{aligned}
& \left[\frac{K_m U_h \operatorname{tg} U_h}{l_h k_h^2} + \frac{U_s \operatorname{tg} U_s}{l_s k_s^2} \right] \left[\frac{K_e U_h}{k_h^2 l_h \operatorname{tg} U_h} + \frac{U_s}{k_s^2 l_s \operatorname{tg} U_s} \right] \\
& + \left(\frac{hc_s m \pi}{\omega d} \right)^2 \left(\frac{1}{k_s^2} - \frac{1}{k_h^2} \right)^2 = 0
\end{aligned} \tag{14}$$

Wherein $K_e = \frac{\varepsilon_h}{\varepsilon_s}$ and $K_m = \frac{U_h}{U_s}$, and defining real auxiliary variables V_h, V_s by

$$V_h = \left[\left(\frac{\omega^2}{c_h^2} \right)^2 - h^2 - \left(m \frac{\pi}{d} \right)^2 l_h \right]^{1/2} \tag{15a}$$

$$V_s = [(m \frac{\pi}{d})^2 + h^2 - \omega^2 \frac{l_s}{c_s^2}]^{1/2} \quad (15b)$$

The factored characteristic equations for the cut-off frequency as obtained from equation (14) are:

$$(\frac{V_s th V_s}{k_s^2} l_s) - K_m V_h \frac{tg V_h}{l_h k_h^2} = 0 \quad (16)$$

$$(\frac{V_s}{k_{ss}^{2l} th V_s}) + K_e \frac{V_h}{k_h^{2l} tg V_h} = 0 \quad (17)$$

where $tg = \tan$, $th = \tanh$

In Eq.(14), on determination of the cut-off frequency through imposition of $h = 0$, the second term disappears and Eqs.(10) can be factored into two simpler equations. V_s in Eqs.(16) and (17) cannot be real for $h = m = 0$. No single hyperbolic mode characterized by $m = 0$ can be propagated. By use of trial frequencies in Eqs.(16) and (17), we can find the cut-off frequency for $m = h = 0$. A fortran program for this calculation is shown in Appendix A. The cut-off frequency for the shielded coplanar line (SCPL) having dimensions shown in Table 1 was found to be 6.8 Ghz.

Table 1. CONFIGURATION DATA IN SCPL

dimension	data(mm)
D	22.86
l_h	2.54
l_s	7.62
ϵ_r	2.2

Dimensions are shown in Table 1 Symbols refer to Fig.2 as follows

D : width of shield

l_h : thickness of substrate

l_s : height of air

ϵ_r : dielectric constant

III. COMPUTER PROGRAM CONSTRUCTION

A. CURRENT DISTRIBUTIONS

In actual computations for the dominant mode, the strip current densities \tilde{J}_{z1} and \tilde{J}_{x1} have been chosen to have physically plausible distributions, as shown in Fig.3, for the continuous strip which has width of $2a$ and length of $2l_1$.

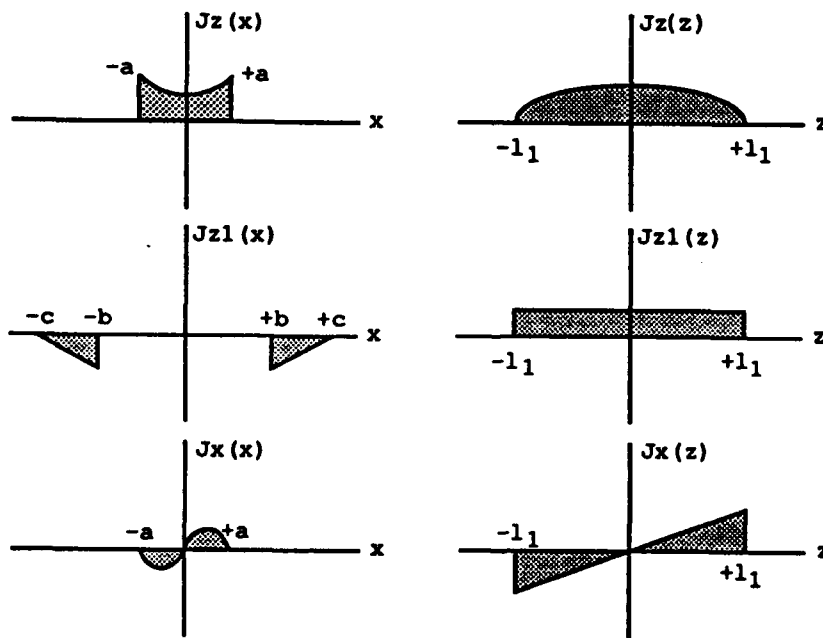


Figure 3. Form of assumed current distributions

Where $2a = A$, $2b = B$, $2c = C$, $2l_1 = l$ (see Fig. 1).

The coordinate forms of the current distributions in Fig.3 are:

$$J_z(x) = \frac{1}{2a} (1 + |\frac{x}{a}|^3) \quad (18a)$$

$$J_{z1}(x) = \begin{cases} \frac{x-b}{2(c-b)} & x > 0 \\ \frac{-x+b}{2(c-b)} & x < 0 \end{cases} \quad (18b)$$

$$J_z(z) = \frac{1}{l_1} \cos \frac{(\pi z)}{2l_1} \quad (18c)$$

$$J_{z1}(z) = \frac{1}{2rl} \quad |z| > \frac{rl}{2} \quad (18d)$$

$$J_x(x) = \frac{1}{a} \sin \frac{\pi x}{a} \quad (18e)$$

$$J_x(z) = \frac{z}{2l_1^2} \quad (18f)$$

Fourier transforms of these current densities are:

$$\tilde{J}_z(k_n) = \frac{2 \sin(k_n a)}{k_n a} + \frac{3}{(k_n a)^2} [HWN] \quad (19a)$$

$$[HWN \equiv \cos(k_n a) - 2 \sin \frac{(k_n a)}{k_n a} + 2(1 - \cos(k_n a) \frac{1}{(k_n a)^2}]$$

$$\begin{aligned} \tilde{J}_{z1}(k_n) &= \left(\frac{1}{b-c} \right) \left(\frac{2}{k_n} \right) [b \sin(k_n b) - c \sin(k_n c)] \\ &+ \left(\frac{1}{b-c} \right) \left[\frac{2}{k_n} (\cos(k_n b) - \cos(k_n c)) \right] \end{aligned} \quad (19b)$$

$$\tilde{J}_z(\beta_m) = \frac{4\pi \cos \beta_m l_1}{\pi^2 - (2\beta_m l_1)^2} \quad (20a)$$

$$\tilde{J}_{z1}(\beta_m) = \frac{\sin(\beta_m l)}{\beta_m l} \quad (20b)$$

$$\tilde{J}_x(k_n) = \frac{2\pi \sin(k_n a)}{(k_n a)^2 - \pi^2} \quad (20c)$$

$$\tilde{J}_x(\beta_m) = \frac{\cos(\beta_m l)}{\beta_m l_1} - \frac{\sin(\beta_m l_1)}{\beta_m l_1^2} \quad (20d)$$

And then, forming products of the x- and z- dependent factors,

$$\tilde{J}_z(k_n, \beta_m) = \tilde{J}_z(k_n) \cdot \tilde{J}_z(\beta_m) + \tilde{J}_{z1}(k_n) \cdot \tilde{J}_{z1}(\beta_m) \quad (21a)$$

$$\tilde{J}_x(k_n, \beta_m) = \tilde{J}_x(k_n) \cdot \tilde{J}_x(\beta_m) \quad (21b)$$

B. COMPUTATION PROCEDURE

1. Change of Transform Variable

In the present work, the strip line resonator was fully enclosed in a metal shield. This permitted the use of a finite Fourier transform rather than the integral transform which is typical of the infinite-line calculations.

The inner products can then be carried out as truncated summation, saving much computer time [Ref.9].

$$\sum_{n=-\infty}^{\infty} \int_{-\infty}^{\infty} \rightarrow \sum_{n=-\infty}^{\infty} \sum_{m=-\infty}^{\infty}$$

In the products, the lower limits are $n = -\infty, m = -\infty$, unless symmetry holds, in which case the sum is:

$$\sum_{m=-\infty}^{\infty} = \sum_{m=0}^{\infty} + 2 \cdot \sum_{m=1}^{\infty}$$

The wave numbers used for the two summations are:

$$k_n = \frac{(n - \frac{1}{2})\pi}{a}, \quad x - \text{direction}$$

$$\beta_m = \frac{(m - \frac{1}{2})\pi}{rl}, \quad z - \text{direction}$$

As shown in Tables 2 and 3, a summation over n of 20 terms is enough, and for the summation over m , 1000 terms leads to convergence within 1 MHz error which is negligible in comparison with the resonant frequency.

Table 2. VARIATION OF NUMBER OF TERMS N

n	m	f_o Ghz
10	1000	3.318
20*	1000	3.3289
40	1000	3.3287

Table 3. VARIATION OF NUMBER OF TERMS M

n	m	f_o Ghz
20	100	3.23
20	500	3.317
20	1000*	3.328
20	1500	3.3287

C. CALCULATION OF FRINGING CAPACITANCE

Two equivalent representations of the electrical effects due to the fringing electromagnetic fields at the open ends of the strip transmission line section are available:

(a.) The stored energy in the fringing fields may be given an equivalent-circuit representation in the form of a small capacitance, ΔC , which is connected from the physical terminations of the line to ground.

(b.) The effect of the open end discontinuity may also be represented by assuming that the length of the open-ended strip is increased by the addition of length increment Δl to each end.

The two foregoing representations are related by the assumption that: $\Delta C = \Delta l C$, where C is the capacitance per unit length of the strip transmission line. Therefore in the present work it is necessary to determine

either ΔC or Δl , from the calculated resonance frequency of the strip resonator. Two methods are available for finding Δl or ΔC from resonance data: (1.) The half-wavelength resonator assumption, and (2.) the terminated transmission-line model for resonance of the open-ended strip.

1. HALF-WAVELENGTH RESONATOR ASSUMPTION

It is assumed that, at its fundamental resonance, the open-ended resonator has a length equal to one half wavelength of the propagating waves on the strip, apart from the perturbation due to the open ends.

The wavelength can be found from a knowledge of the propagation constant $\beta(\omega_o)$, where ω_o is the angular frequency of resonance, i.e., $\lambda_g = \frac{2\pi}{\beta}$. Therefore, $\Delta l = \frac{1}{2} \left(\frac{\lambda_g}{2} - l \right)$ where l is the physical length of the resonator strip and λ_g is the guided wavelength in the strip. In view of the TEM model for the transmission line defined by L (henry/m) and C (farad/m), we have the relations:

$$Z_o = \sqrt{\frac{L}{C}} \quad (22)$$

$$\beta = \frac{\omega}{c} \sqrt{\epsilon_{\text{reff}}} = \sqrt{LC} \omega_o \quad (23)$$

$$v = \frac{1}{\sqrt{LC}} = \frac{c}{\sqrt{\epsilon_{\text{reff}}}} \quad (24)$$

where v is the wave velocity in SCPL, and c is the free-space velocity of light.

By using Eqs.(22) and (23), the capacitance C is defined

$$C = \frac{\beta}{Z_o \omega_o} \quad (25)$$

where C is capacitance/ meter of the transmission line, and Z_o is its characteristic impedance.

Therefore the fringing capacitance ΔC is

$$\Delta C = \Delta I C = \frac{1}{2} \left(\frac{\lambda_g}{2} - l \right) \frac{\beta}{Z_o \omega_o} \quad (26)$$

2. TERMINATED TRANSMISSION-LINE MODEL

It is assumed that the impedance seen looking from the center of the strip toward the open end has a zero value at the resonance of the strip resonator. This impedance can be calculated from the expression for the input impedance of a section of transmission line of length $\frac{l}{2}$, terminated by impedance Z_c (see Fig. 4):

$$Z_{in} = \frac{Z_c + jZ_o \tan(\beta \frac{l}{2})}{Z_o + jZ_c \tan(\beta \frac{l}{2})} Z_o \quad (27)$$

Where Z_o is the characteristic impedance of the line.

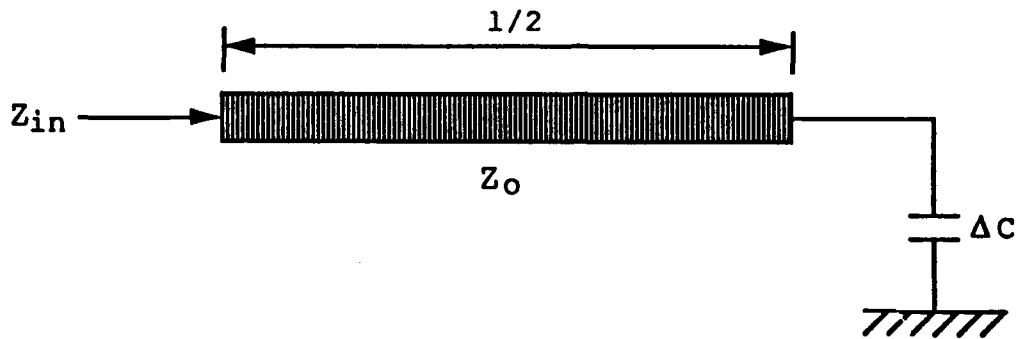


Figure 4. Terminated transmission line model

In the present case,

$$Z_c = \frac{1}{j\omega_o \Delta C} \quad (28)$$

$$\Delta C = \frac{1}{\omega_o Z_o} \cot\left(\beta \frac{l}{2}\right) \quad (29)$$

A plot of Eq (27), as a function of trial values of ΔC is shown in Fig.5.

With the value of ω_o at resonance known, a CAD program may be used to determine the value of ΔC which leads to a zero of $|Z_{in}|$.

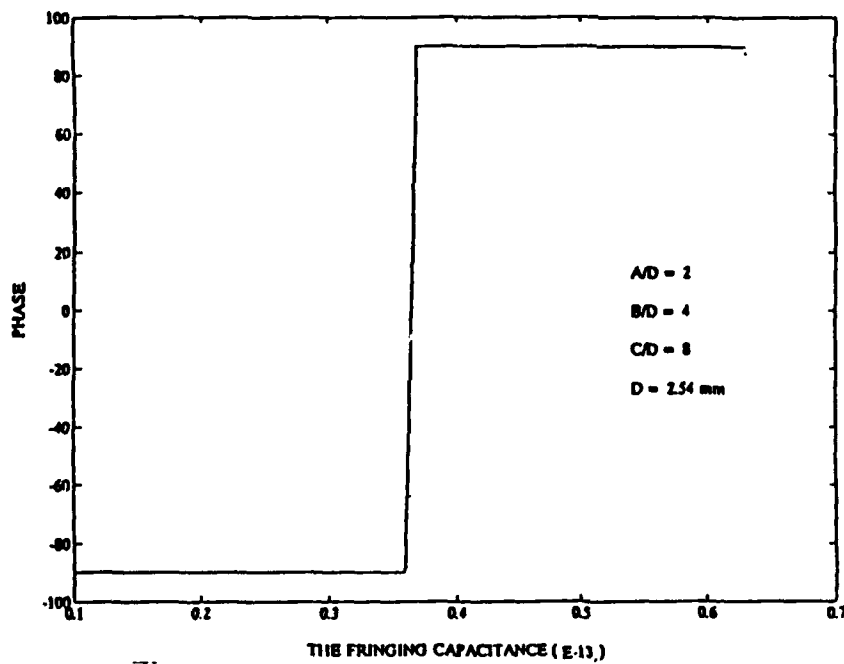
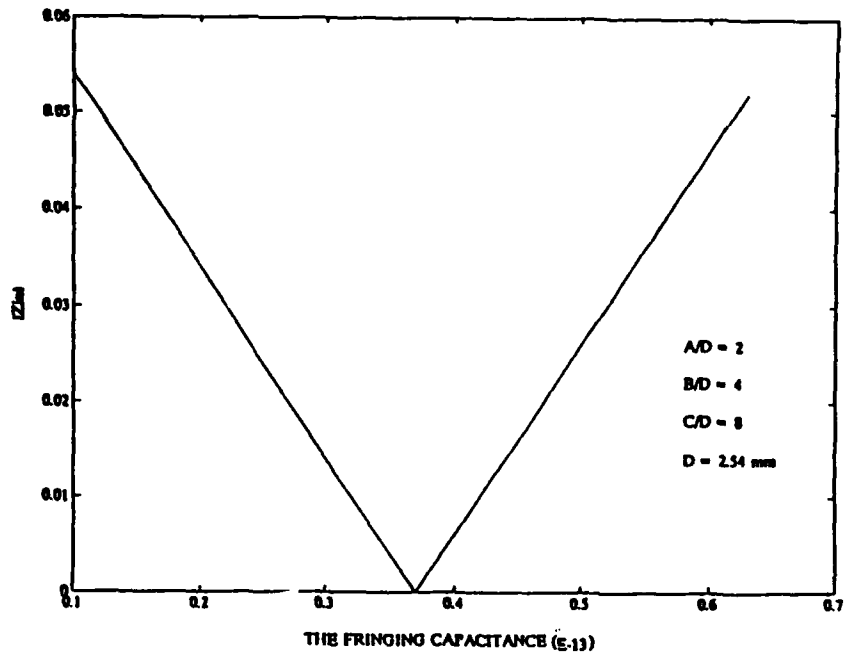


Figure 5. Magnitude and Phase of Z_m for terminated line - segment

IV. RESULT OF COMPUTATION

A. SCPL WITH VARYING DIELECTRIC CONSTANT

In Fig.6, A , B , and C were held fixed, and ϵ_r was increased from 2.2 to 4.0 and 10.0. The effect on ΔC , $\epsilon_{r_{eff}}$, and Z_o and resonant frequency, f_o , was investigated. The value of ΔC is obtained by the two methods described above.

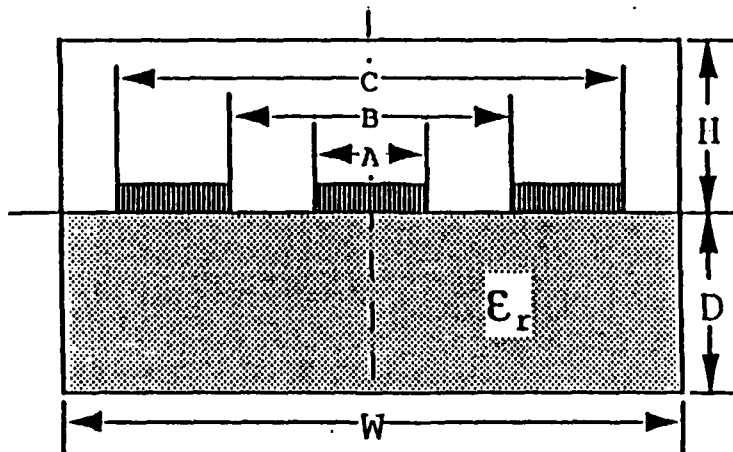


Figure 6. Cross section view of SCPL

Table 4. CONFIGURATION DATA IN SCPL

dimensions	data(mm)
A	5.08
B	10.16
C	20.32
W	22.86
H	7.62
D	2.54

Figure 7 shows that the anticipated effect is obtained. An increase of ϵ_r causes the fringing capacitance to increase and resonant frequency, f_o , to decrease. In Fig.8, the increasing ϵ_r causes Z_o to decrease, and ϵ_{reff} to increase. The calculation of ϵ_{reff} by the variational method or the alternate method of moments returns nearly the same value. Again, the results are consistent with the expected predictions.

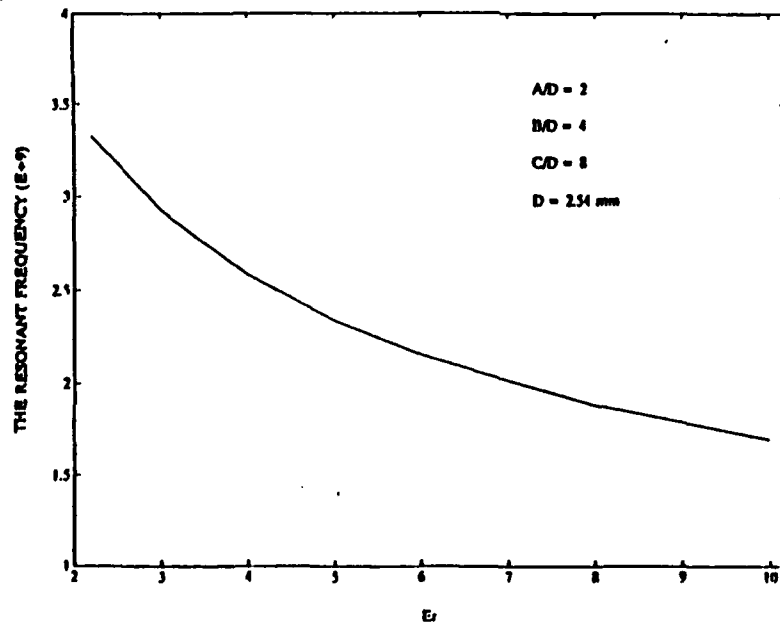
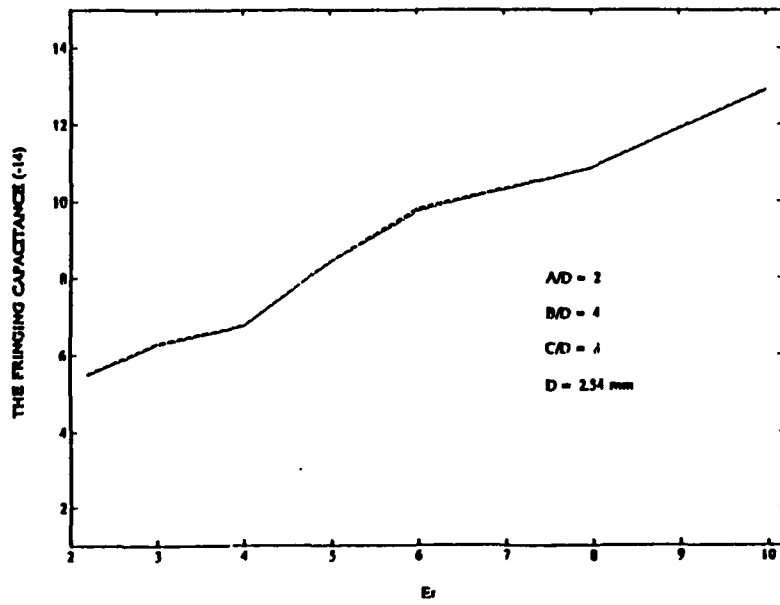


Figure 7. ΔC and f_r versus ϵ_r in SCPL

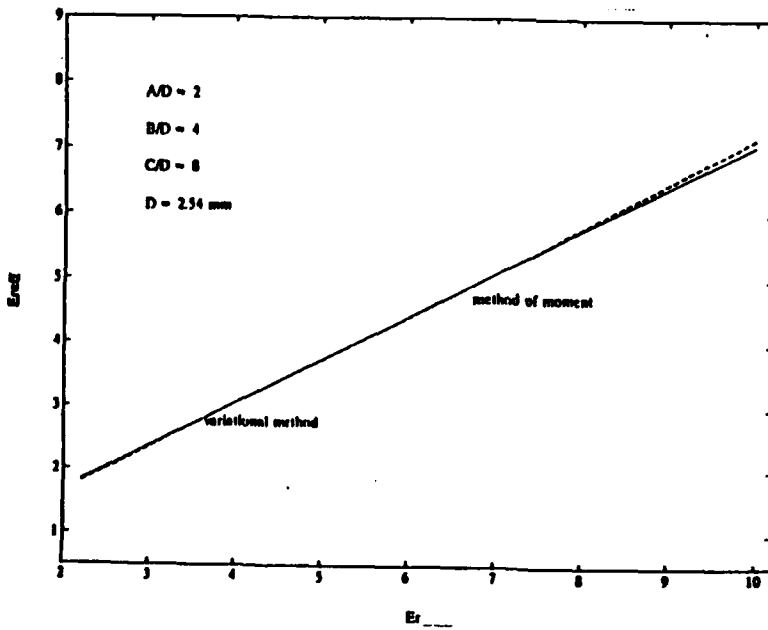
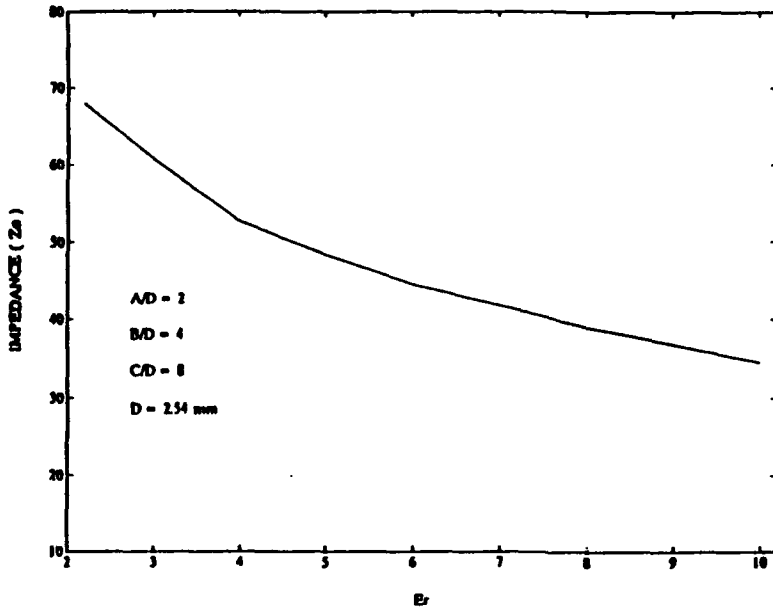


Figure 8. Z_0 and ϵ_{rod} versus ϵ_r in SCPL

B. SCPL WITH VARYING CONDUCTOR SPACING

In Fig.6, the values A, D, H, GW remain fixed while the gaps between the center and ground conductors are increased (where GW is the ground-plane width). The effects on ΔC , ϵ_{reff} , and Z_o was analyzed. The increase of the gaps as shown in Fig.9 illustrates that resonant frequency, f_o , and ΔC remain relatively constant, independent of the SCPL gap width. Figure 10 shows a slight increase in impedance, Z_o , and in ϵ_{reff} with increase of gap width.

Table 5. CONFIGURATION DATA IN SCPL

dimension	data(mm)
D	2.54
H	7.62
A	2.54
GW	2.54
ϵ_r	2.2

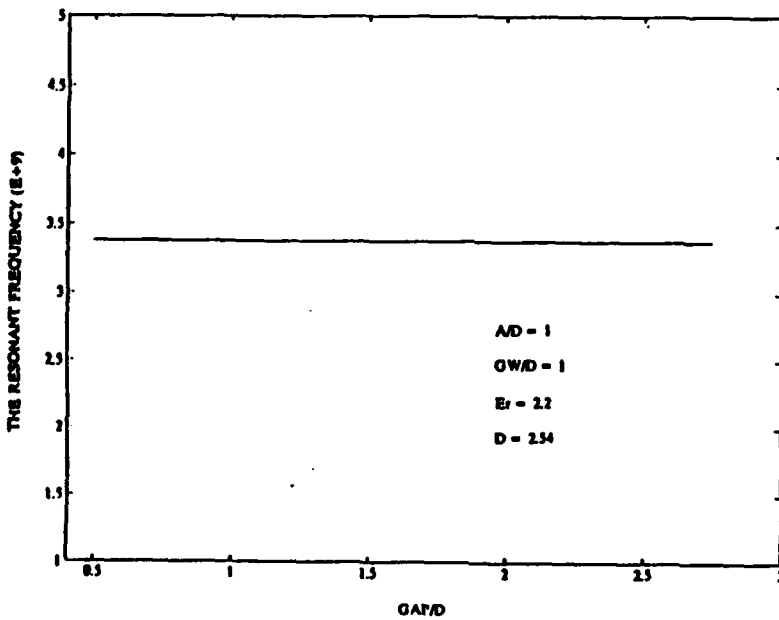
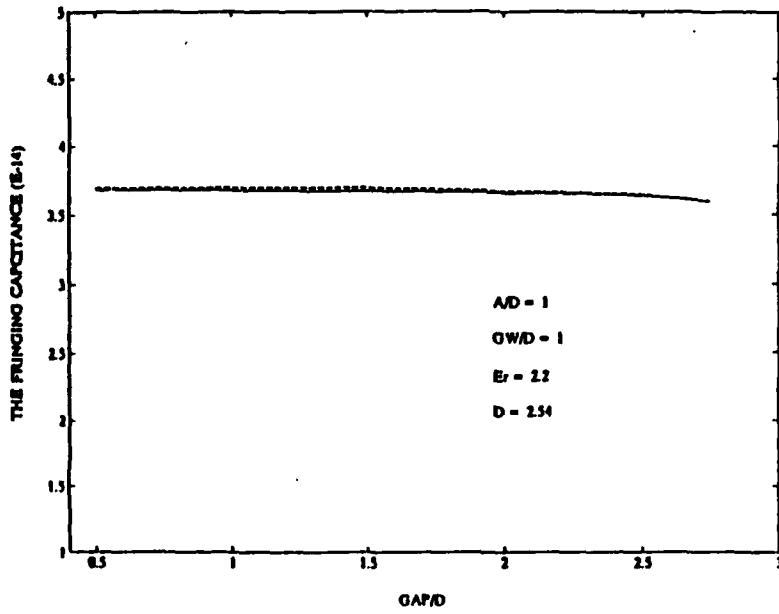


Figure 9. ΔC and f_c versus GAP/D in SCPL

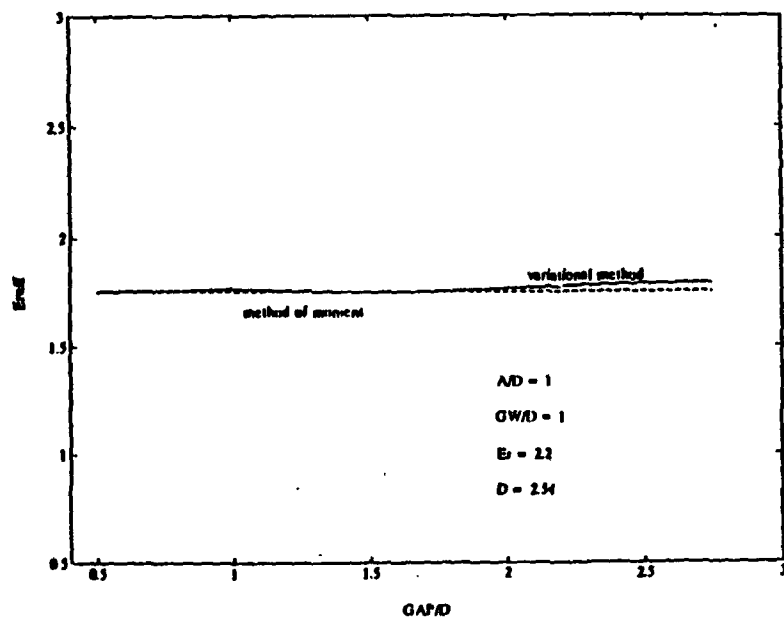
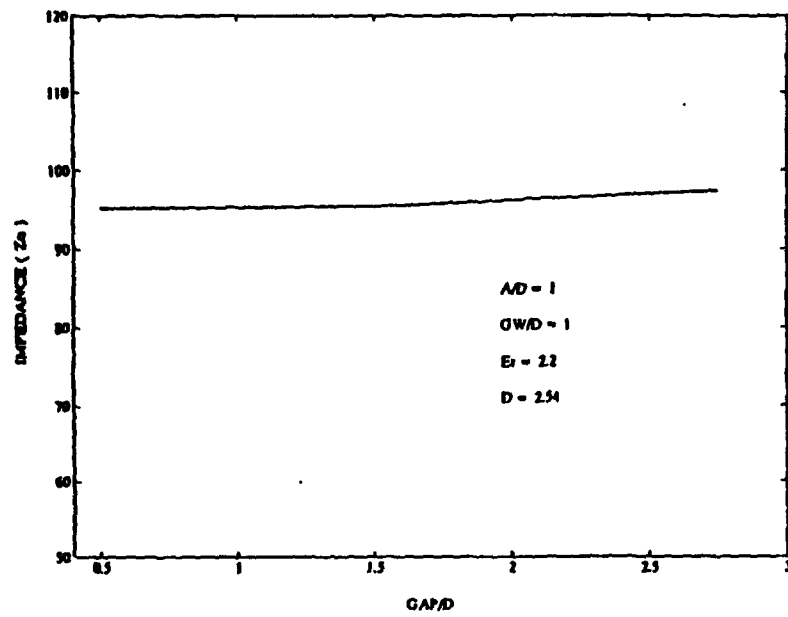


Figure 10. Z_0 and ϵ_{eff} versus GAP/D in SCPL

C. SCPL WITH VARYING WIDTH OF THE CENTER CONDUCTOR

In Fig.6, the ground plane widths and values for H , D , W , ϵ_r are fixed. Only the width A of the center conductor is varied. This change necessarily changes the gap width also. The changing gap caused ΔC , f_o , ϵ_{reff} , and Z_o to change as will be discussed. The increasing width caused ΔC to decrease abruptly until $A/D = 1$. Above this ratio, ΔC increases slowly. Figure 11 illustrates that resonant frequency, f_o , increases until A/D is equal to 1. Above this ratio f_o remains relatively constant. In Fig.12, the increased width caused Z_o to decrease, and ϵ_{reff} remains relatively constant.

Table 6. CONFIGURATION DATA IN SCPL

dimensions	Data(mm)
W	22.86
GW	5.08
D	2.54
H	7.62
ϵ_r	2.2

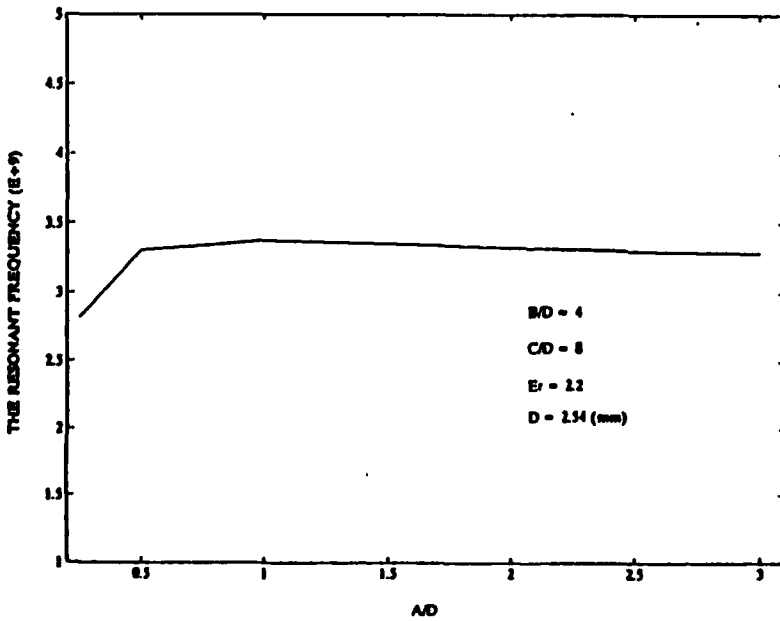
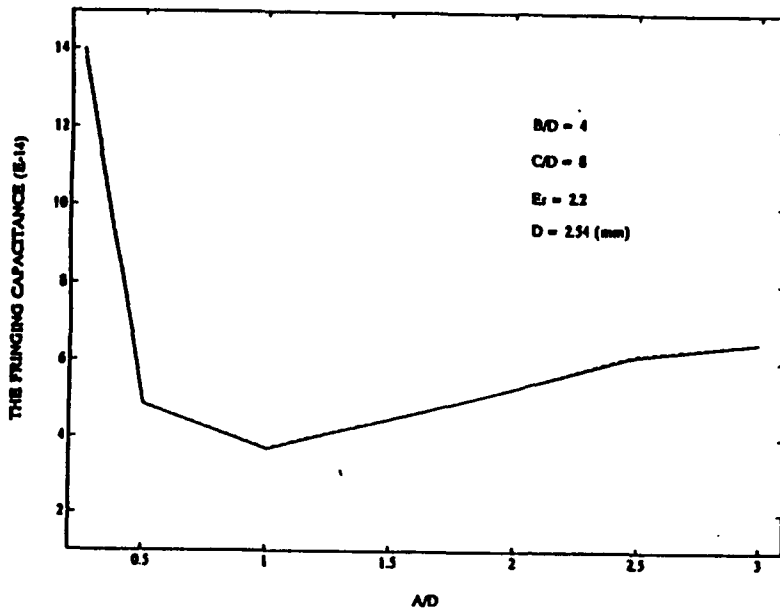


Figure 11. ΔC and f_r versus A/D in SCPL

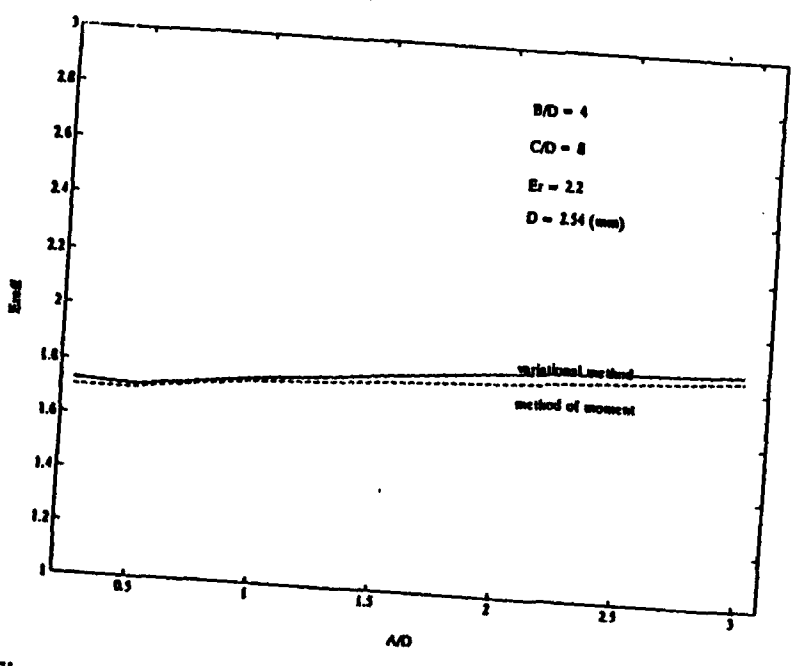
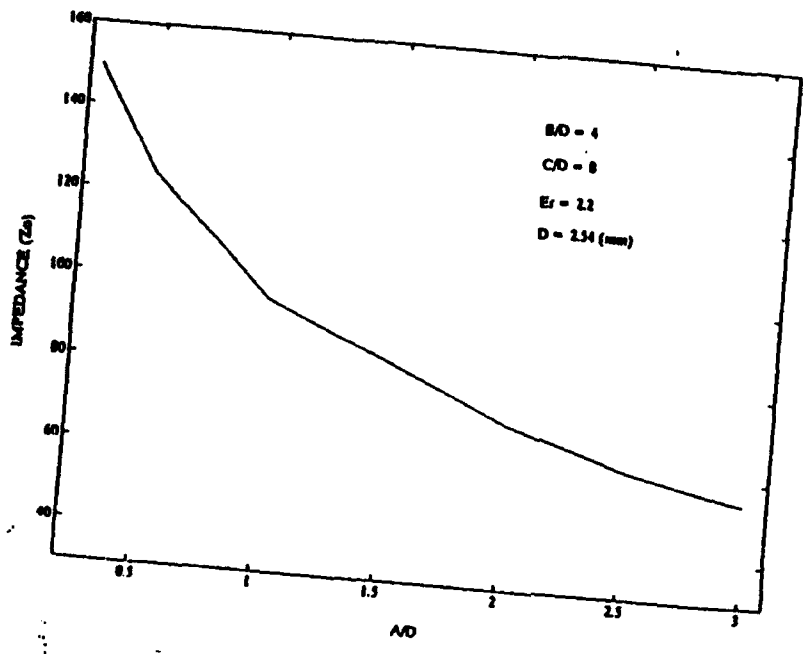


Figure 12. Z_o and s_{ref} versus A/D in SCPL

D. SCPL WITH VARYING HEIGHT OF DIELECTRIC LAYER.

In Fig.6, A, B, C, and ϵ_r remain fixed while the dielectric layer height is increased from 1.27 to 6.35 mm . The effect on ΔC , ϵ_{reff} , and Z_o was investigated. Figure 13 shows that increasing D causes resonant frequency, f_o , to increase and the fringing capacitance, ΔC , to decrease slightly. Figure 14 shows that the increasing D causes Z_o to increase and ϵ_{reff} to decrease slightly.

Table 7. CONFIGURATION DATA IN SCPL

dimensions	Data(mm)
A	5.08
B	10.16
C	20.32
ϵ_r	2.2

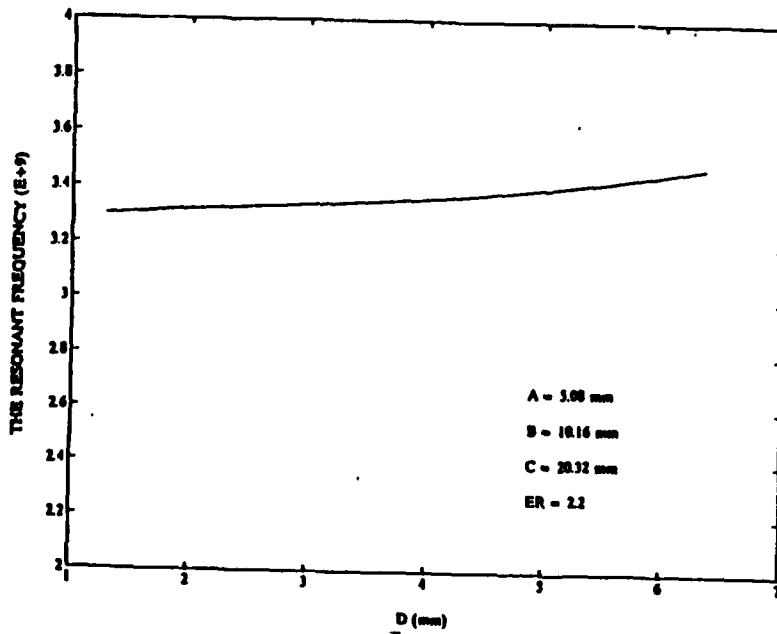
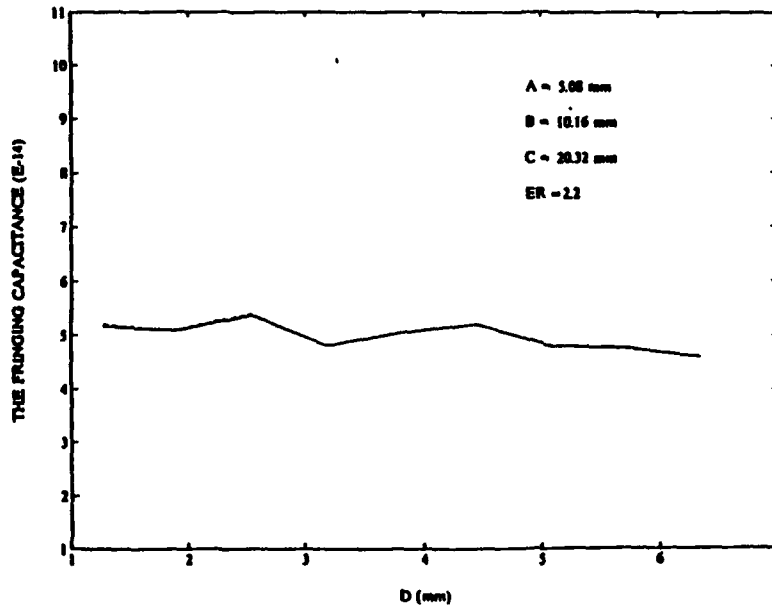


Figure 13. ΔC and f_0 versus D in SCPL

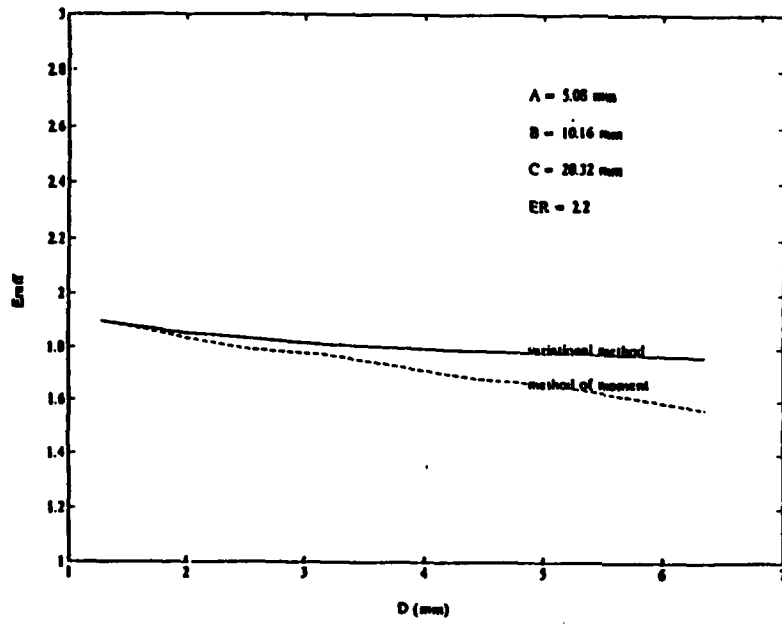
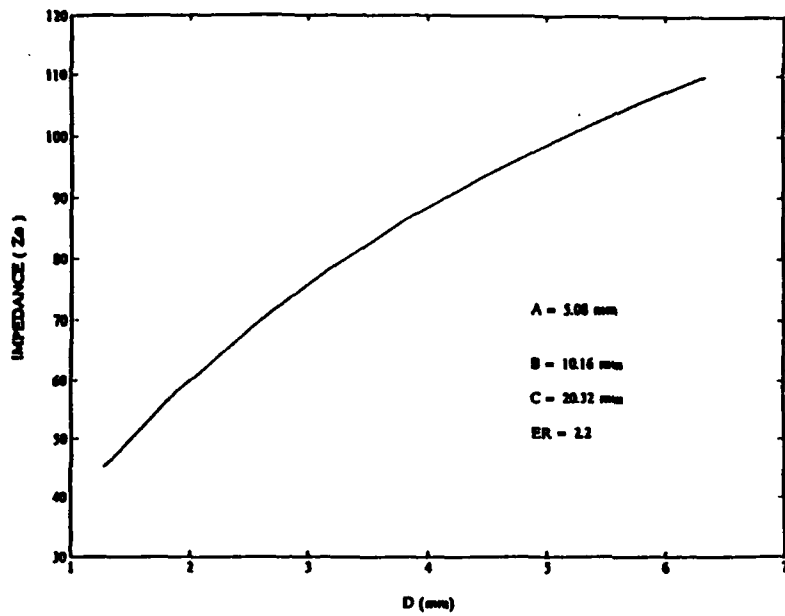


Figure 14. Z_0 and ϵ_{eff} versus D in SCPL

V. CONCLUSION

This thesis follows the methods originated by Itoh for the analysis of the shielded micro strip resonator. A fully-shielded enclosure was employed, allowing the use of a finite Fourier transform in two coordinates. This change reduced the computation time significantly, while producing accuracy comparable with that obtained using the integral transform along the line axis. Also it should be mentioned that the operating frequency in the paper was taken to be below the cut-off frequency of SCPL, as verified by the thesis in Chapter II. The perturbed-resonator technique permitted the use of the strip current density distributions suggested by Itoh, and the ground strip current density distributions appropriate to the present work. These are known to give accurate results in Galerkin's method. The numerical values of open-end capacitances were obtained from two resonator models, and found to be in good agreement. In summary, values of the circuit model for the open-end discontinuity in shielded coplanar line has been investigated.

APPENDIX A. FORTRAN PROGRAMS

A. RESONANT FREQUENCY

```

INTEGER I,N,M,COMPARE,COUNT
REAL W,A1,A2,L,U,H,ER,F,R,P,L1,L2
REAL KN,BETA,OMEGA,RL,Q
REAL P1,F0,MUO,C
REAL GAM1,GAM2S
REAL JZIN,JZKN1,JZKN2,JZBE1,JZBE2,JZBE3,JZ,JZ1,JZ2,JZ3
REAL JXKN1,JXKN2,JXUE1,JXBE2,JX1,JX2,JX,JZKN3,JZOE4,JZ4
REAL CMP,LIMIT,U_OF,NEWF,LIMF
DOUBLE PRECISION DCMP

C
LOGICAL LLOG

C
COMPLEX*8 GAM1,GAM2,RTH1,RTH2
COMPLEX*8 ZEO
COMPLEX*8 ZZ,ZXX,ZX7,ZZX
COMPLEX*8 K11,K12,K22,J,SK11,SK12,SK22,DET
CHARACTER*9 FNAME
CHARACTER*12 SNAME
Q=0.04
OPEN(1,FILE='CXXXX')
PRINT*, 'ENTER OUTPUT DATA FILE NAME FN'
READ*, FNAME
OPEN(2,FILE=FNAME)
SNAME=FNAME//'.PLT'
OPEN(3,FILE=SNAME)
WRITE(2,*) ' FILE NAME = ',FNAME
WRITE(3,*) ' FILE NAME = ',SNAME

C
PARAMETER
C=1.FU
J=CMPLX(0.,1.)
PI=4.*ATAN(1.)
F0=1.E-9/(36.*PI)
MUO=4.*PI*1.E-7
LIMIT=1.E-2
COMPARE=1
COUNT=1
LLOG=.TRUE.

C
CALL READ(A1,A2,L1,L2,W,U,P,D,H,ER)

C
WRITE(2,22) A1,A2,L1,L2,W,D,P,D,H,ER
22 FORMAT(13,'UNIT : METER')
* //,13,'COPLANAR LINE WIDTH AND LENGTH : ',2(F9.7,2X)
* //,13,'COPLANAR LINE LENGTH L1,L2 : ',2(F9.7,2X)
* //,13,'RESONATOR WIDTH : ',F9.5
* //,13,'INSIDE AND OUTSIDE WIDTH : ',2(F9.7,2X)
* //,13,'HEIGHTS OF LAYERS 1 AND 2 : ',2(F9.7,2X)
* //,13,'PERMITTIVITY OF SUBSTRATE ER : ',F9.5)
PRINT*, 'ENTER THE NUMFR OF OUTER SUM LOOP N = '
READ*, N
N=20
WRITE(2,*) 'THE NUMBER OF OUTER SUM LOOP N = ',N
WRITE(3,*) 'THE NUMBER OF OUTER SUM LOOP N = ',N

```

```

PRINT*, 'ENTER THE NUMBER OF INNER SUM LOOP  'M = '
READ*, M
M=20, 40, 100, 500, 1000, 2000, 3000, 4000 ETC.
WRITE(2,*) 'THE NUMBER OF INNER SUM LOOP  'M = ',M
WRITE(3,*) 'THE NUMBER OF INNER SUM LOOP  'M = ',M

C
L=L1*L2
RL=5.*_

C
C
I
PRINT*, 'ENTER BOUNDARY FREQUENCY (GHZ)'
READ*,F
F=F*1.E9

C
II
PRINT*, 'FREQUENCY = ',F
WRITE(6,*) 'FREQUENCY = ',F

C
OMEGA=2.*PI*F

C
K11=CMPLX(0.,0.)
K12=CMPLX(0.,0.)
K22=CMPLX(0.,0.)
DO 20 I=1,N
  KY=(I-.5)*PI/d

C
  J7IN=COS(KN*A1)-2.*SIN(KN*A1)/(KN*A1)+2.*(1.-COS(KN*A1))/
  (KN*A1)**2
  J7KN1=2.*SIN(KN*A1)/(KN*A1)+3.*J7IN/(KN*A1)**2
  J7IN1=COS(KN*A2)-2.*SIN(KN*A2)/(KN*A2)+
  2.*(1.-COS(KN*A2))/(KN*A2)**2
  J7KN2=2.*SIN(KN*A2)/(KN*A2)+3.*J7IN1/(KN*A2)**2
  J7KNJ=Q*(1./(n-p)*(2./KN)*(R*SIN(KN*B)-P*SIN(KN*U))
  +1./(n-p)*(2./KN)*(COS(KN*B)-COS(KN*P)))

C
  JXKN1=-2.*PI*SIN(KN*A1)/(P1**2-(KN*A1)**2)
  JXKN2=-2.*PI*SIN(KN*A2)/(P1**2-(KN*A2)**2)
  SK11=CMPLX(0.,0.)
  SK12=CMPLX(0.,0.)
  SK22=CMPLX(0.,0.)
  DO 40 IM=1,M
    BETA=(REAL(IM)-.5)*PI/RL

C
C
  GAM1S=KN**2+BETA**2-E0*MU0*ER*OMEGA**2
  CALL GAMCT(GAMA1,GAM1S,RTH1,D)

C
  GAM2S=KN**2+BETA**2-E0*MU0*OMEGA**2
  CALL GAMCT(GAMA2,GAM2S,RTH2,H)

C
  ZED=(RTH1+ER*RTH2)*(GAMA1**2/RTH1+GAMA2**2/RTH2)

C
  ZXZ=KN*BETA*(RTH2+RTH1)/ZED
  ZZ7=[(KN**2-GAMA1**2)*RTH2+(KN**2-GAMA2**2)*RTH1]/Z
  ZXX=[(KN**2-GAMA1**2)*RTH2+(BETA**2-GAMA2**2)*RTH1]

```

```

C
      ZZX = ZXZ
      JZDE3 = SIN(BETA*L2)/(BETA*L2)
      JZDE4 = SIN(BETA*RL)/(BETA*RL)
C
C
      JZDE1 = 4.*PI*COS(BETA*(L1))/(PI**2-(2.*BETA*(L1))**2)
      JZDE2 = 4.*PI*COS(BETA*(L2))/(PI**2-(2.*BETA*(L2))**2)
      JZ2 = JZKN2*JZDE2
      JZ1 = JZKN1*JZDE1
      JZ4 = JZKN3*JZDE4
C
      JZ = 0.5*(JZ1+JZ2)+JZ4
      JXDE1 = COS(BETA*(L1))/(BETA*(L1))
      - SIN(BETA*(L1))/(BETA*(L1))**2
      JXDE2 = COS(BETA*(L2))/(BETA*(L2))
      - SIN(BETA*(L2))/(BETA*(L2))**2
      JX1 = JXKN1*JXDE1
      JX2 = JXKN2*JXDE2
C
      JX = 0.5*(JX1+JX2)
C
      SK11 = SK11+JZ*ZZZ*JZ
      SK12 = SK12+JZ*ZZX*JX
      SK22 = SK22+JX*ZXX*JX
40  CONTINUE
      K11 = K11+SK11
      K12 = K12+SK12
C
      K22 = K22+SK22
70  CONTINUE
      PRINT*, 'ZXX', ZXX, 'ZZX', ZZX
C
      PRINT*, JX1, JX2, JX
      PRINT*, JZ1, JZ2, JZ3, JZ
      PRINT*, ZZZ, ZZX, ZXX
C
      PRINT*, 'JX1', JX1, 'JX2', JX2, 'JXDE1', JXDE1
      PRINT*, 'CHECK K11 = ', K11
      WRITE(2,*) 'CHECK K11 = ', K11
      PRINT*, 'CHECK K12 = ', K12
      WRITE(2,*) 'CHECK K12 = ', K12
      PRINT*, 'CHECK K22 = ', K22
      WRITE(2,*) 'CHECK K22 = ', K22
      DET = K11*K22 - K12*K12
      PRINT*, 'DET = ', DET
      WRITE(2,*) 'DETERMINANT = ', DET
C
      CALL FDSORT(F, DET, COUNT)
      COUNT = COUNT + 1

```

```

C
C
IF (LLDG) THEN
  PRINT*, 'MAKE SURE OPPOSITE SIGNS BETWEEN 1ST & 2ND DEFS'
  PRINT*, 'IF SAME SIGNS THEN ENTER 9 , OR ENTER 0'
C
  READ*, IJK
  IF (IJK.EQ.9) THEN
    OLDF=F
    GOTO 1
  ENDIF
  LLDF=.FALSE.
ENDIF
ENDIF

C
C
CMP=REAL(DEF)
DCMP=DOUBLE(CMP)
LIMF=ABS(F-OLDF)
C
  PRINT*, 'CHECK LIMIT FREQ ',LIMF
  WRITE(7,*) 'CHECK LIMIT FREQ = ',LIMF
C
  IF (ABS(DCMP).GT.LIMIT.AND. LIMF.GT.1.E4) THEN
    CALL SIVAL(DCMP,OLDF,F,NEWF,COMPARE)
    OLDF=F
    F=NEWF
    GOTO 11
  ENDIF
C
  PRINT*, 'RESONANCE FREQUENCY = ',F
  WRITE(2,*) 'RESONANCE FREQUENCY = ',F
C
  CALL FDSORT(F,DEF,100)

  STOP
  END

```

```

C*****
SUBROUTINE READF(A1,A2,L1,L2,W,B,P,D,H,ER)
REAL A1,A2,L1,L2,W,B,P,D,H,ER
INTEGER DDDD
9 PRINT*, 'DATA INPUT : KEYWORD(ENTER "I"), FILE(ENTER "O")'
READ*, DDDD
IF (DDDD.EQ.0.OR.DDDD.EQ.0) THEN
  READ(1,*) A1,A2,L1,L2,W,B,P,D,H,ER
ELSE IF (DDDD.EQ.1.OR.DDDD.EQ.1) THEN
  PRINT*, 'ENTER THE 1,2 WIDTH IN MM'
  READ*, A1,A2
  PRINT*, 'ENTER THE LENGTH OF MICRO STRIP LINE IN MM'

```

```

      READ*,L1,L2
      PRINT*, 'ENTER THE WIDTH OF RESONATOR'
      READ*,W
      PRINT*, 'ENTER INSIDEWIDTH AND OUTSIDEWIDTH'
      READ*,D,P
      PRINT*, 'ENTER THE HEIGHT OF LAYERS 1 AND 2'
      READ*,D,H
      PRINT*, 'ENTER THE PERMITTIVITY ER OF SUBSTRATE LAYER'
      READ*,ER
    ELSE
      PRINT*, 'SELECT "1" OR "0"'
      GO TO 2
    ENDIF

    PRINT 32, A1,A2,L1,L2,W,B,P,D,H,ER
    WRITE (2,32) A1,A2,L1,L2,W,B,P,D,H,ER
    A2= A2*1.E-3
    A1= A1*1.E-3
    L1=L1*1.E-3
    L2=L2*1.E-3
    W = W*1.E-3
    B = B*1.E-3
    P = P*1.E-3
    D = D*1.E-3
    H = H*1.E-3
    ER=ER*1.0
32  FORMAT(13, 'UNIT: MILLIMETER'
+ //,TJ, 'MICRO STRIP LINE 1,2 WIDTH          :',2(F9.7,3X)
+ //,TJ, 'MICRO STRIP LINE WIDTH L1,L2        :',2(F8.3,3X)
+ //,TJ, 'RESONATOR WIDTH                      :',F9.5
+ //,TJ, 'INSIDE AND OUTSIDE WIDTH            :',2(F9.5,3X)
+ //,TJ, 'HEIGHT OF LAYERS 1,2                :',2(F9.5,3X)
+ //,TJ, 'PERMITTIVITY OF SUBSTRATE ER        :',F9.3)
    RETURN
  END
C*****
SUBROUTINE GAMC1(GAMA,GAMS,CT,LENGTH)
COMPLEX*8 GAMA,CT
REAL GAMS,LENGTH,GAMR,CTR
GAMR = SQRT(ABS(GAMS))
IF(GAMS.LT.0.) THEN

  GAMA = CMPLX(0.,GAMR)
  CTR = -GAMR*TAN(GAMR*LENGTH)
  CT = CMPLX(CTR,0.)
ELSE
  GAMA = CMPLX(GAMR,0.)
  CTR = GAMR*TANH(GAMR*LENGTH)
  CT = CMPLX(CTR,0.)

ENDIF
RETURN
END

```

```

*****
SUBROUTINE SLVAL(FUN,OXV,XV,NEWXV,SN)
INTEGER SN
REAL OXV,XV,NEWXV,POSXV,NEGXV
DOUBLE PRECISION FUN
IF(SN.EQ.1) THEN
  IF(FUN.GT.0) THEN
    POSXV = XV
    NEGXV = OXV
  ELSE
    NEGXV = XV
    POSXV = OXV
  ENDIF
  NEWXV = (POSXV + NEGXV)/2
  SN = SN + 2
ELSE
  IF(FUN.GT.0) THEN
    POSXV = XV
  ELSE
    NEGXV = XV
  ENDIF
  NEWXV = (POSXV + NEGXV)/2
ENDIF
RETURN
END
*****
SUBROUTINE FDSORT(FQY,SDET,ICOUNT)
INTEGER ICOUNT,IC
REAL FREQY(100),FQY,RTEMP,MAGDET,TFQY
COMPLEX*8 DETMT(100),SDET,CTEMP,TSDET
TFQY = FQY
TSDET = SDET
IF(ICOUNT.EQ.1) THEN
  FREQY(1) = TFQY
  DETMT(1) = TSDET
ELSEIF(ICOUNT.NE.100) THEN
  DO 10 I=1,ICOUNT-1
    RTEMP = FREQY(I)
    CTEMP = DETMT(I)
    IF (RTEMP.GT.TFQY) THEN
      FREQY(I) = TFQY
      TFQY = RTEMP
      DETMT(I) = TSDET
      TSDET = CTEMP
    ENDIF
10  CONTINUE
  FREQY(ICOUNT) = TFQY
  DETMT(ICOUNT) = TSDET
  IC = ICOUNT
ELSEIF(ICOUNT.EQ.100) THEN
  WRITE(3,110)
110  FORMAT(//,15,'FREQUENCY ',T20,'MAG OF DET ',T35,'DETERMINANT')
  DO 20 J =1,IC
    MAGDET = SQRT(REAL(DETMT(J))**2+AIMAG(DETMT(J))**2)
    WRITE(3,210) FREQY(J),MAGDET,DETMT(J)
210  FORMAT(15,F15.2,T20,F15.3,T35,2(E15.8))
20  CONTINUE
ENDIF
RETURN
END

```

B. THE FRINGING CAPACITANCE

```

* THIS IS THE PROGRAM OF CALCULATING THE CAPACITANCE
REAL      ZCAP,ZO,BETA,L,ZIN,F,TH,PI
REAL      A,U,T1
INTEGER T
CHARACTER*8 FNAME
PI = 3.14
PRINT*, 'ENTER OUTPUT FILENAME'
READ*, FNAME
OPEN(2, FILE=FNAME)
WRITE(2,*) ' FILE NAME = ', FNAME
* THE PROGRAM OF FINDING TAN(ETA*L)
PRINT*, 'ENTER ETA'
READ*, BETA
PRINT*, 'ENTER L (MM)'
READ*, L
L=L/1000.
PRINT*, 'ENTER RESONANT FREQUENCY F0 (GHZ)'
READ*, F
F=F*1.E9
PRINT*, 'ENTER Z0'
READ*, Z0
TH = TAN(BETA*L)
PRINT*, 'ETA', BETA
PRINT*, 'F', F
PRINT*, 'L', L
PRINT*, 'Z0', Z0
* FINDING THE ZIN VALUE
WRITE(2,110)
110  FORMAT(//, T5, ' TH', T20, ' ZIN', T35, ' CAPACITANCE')
DO 100 T = 10, 200
    T1=T*1.E-15
    ZCAP=1./(T1*PI*2*F)
    ZIN = (-ZCAP+Z0*TH)/(Z0+(ZCAP*TH))
    PRINT*, 'CF', T1
    PRINT*, 'ZIN', ZIN
WRITE(2,210) TH, ZIN, T1
210  FORMAT(15, F15.2, T20, F15.3, T35, 2(E15.8))
100  CONTINUE
END

```

C. PROPAGATION CONSTANT

```

INTEGER  MMAX,NMAX
REAL  A,D,T,H,PI,ER,FG,OMG,E0,KN,G1S2,B0,B00,DATA,FLAG,AA2,CC,W
REAL  G1,CT01,CT03,GT1,GT3,G2S2,G2,CT02,KE1,KH1,JZ1
REAL  N,OUT,FIN
DIMENSION  U(60),OUT(30)
COMPLEX  GM1,GM3,CT1,CT3,GM2,CT2,DENE,ZE,KE,DENH,ZH,KH
COMPLEX  TRMN,SUMUP,JZ11
C READ*,FNAME
C PI=4.*ATAN(1.)
FLAG=0
MMAX=30
NMAX=30
PRINT*, 'ENTER FREQ.,GHZ.'
C READ*,FG
C PRINT*, 'ENTER SHLD. WOTH(MM) W'
C READ*,AA2
AA2=22.85
A=AA2/2000
C PRINT*, 'ENTER SHLD. HT.(MM) L'
C READ*,LC
CC1=10.16
CC=CC1/1000
U1=1.E-60
D=D1/1000
PRINT*, 'ENTER SCPL THICKNESS(MM) D'
C READ*,T
T1=2.54
T=T/1000
H=CC-(T)
PRINT*, 'ENTER THE SCPL DIELEC. CONST.'
C READ*,ER
ER=4.0
PRINT*, 'ENTER THE LINEWIDTH(MM) 2*W'
C READ*,WW
W=WW/2000
OMG=FG*PI*2E9
E0=8.81E-12
NO=(OMG/3E8)*SQRT((ER+1)/2)
RO=(OMG/3E8)*SQRT(ER*ER)
BO=(OMG/3E8)*SQRT(ER)
C H00=0.20
DATA=0.10
GO TO 1
5 BO=JIN
B00=0.85
DATA=0.0070
4 DO 2 M=1,NMAX
SUMUP=0
P(M)=BO*(B00+M*DATA)
DO 1 N=1,NMAX
KN=(N-0.5)*PI/A

```

```

G1S2=KN**2+U(M)**2-OMG**2/9E16
G1=SQRT(ABS(G1S2))
IF(G1S2.LT.0) THEN
  GM1=CMPLX(0.,G1)
  GM3=GM1
  CT01=-1./TAN(G1*H)
  CT03=-1./TAN(G1*D)
  CT1=CMPLX(0.,CT01)
  CT3=CMPLX(0.,CT03)
ELSE
  GM1=CMPLX(G1,0.)
  GT1=1./TANH(G1*H)
  GM3=GM1
  GT3=1./TANH(G1*D)
  CT1=CMPLX(GT1,0.)
  CT3=CMPLX(GT3,0.)
ENDIF
C
G2S2=KN**2+U(M)**2-EP*OMG**2/9.E16
G2=SQRT(ABS(G2S2))
IF (G2S2.LT.0) THEN

  GM2=CMPLX(0.,G2)
  CT02=-1./TAN(G2*H)
  CT2=CMPLX(0.,CT02)
ELSE
  GM2=CMPLX(G2,0.)
  GT2=1./TANH(G2*H)
  CT2=CMPLX(GT2,0.)
ENDIF
C
DENE=CT2*CT3+CT1*CT3*(GM2/GM1)/ER+CT1*CT2+(GM3/GM2)*ER
ZE=(GM2*CT3)/ER+GM3*CT2/DENE
KE1=-1./(UMG*E0)
KE=CMPLX(0.,KE1)
ZE=KE*ZE
DENH=GM1*CT1+GM2*CT2+GM1*CT1+GM3*CT3+GM2*CT2+GM3*CT3+GM2**2
ZH=(GM2*CT2+GM3*CT3)/DENH
KH1=OMG*PI**4E-7
KH=CMPLX(0.,KH1)
ZH=ZH*KH
JZ1=COS(KN*W)-2*SIN(KN*W)/(KN*W)+2*(1-COS(KH*W))/(KH*W)**2
JZ1=2.*SIN(KN*W)/(KN*W)+3./[(KN*W)**2]*JZ1
JZ11=CMPLX(JZ1,0.)
TRMN=-(U(M)**2*ZE+KN**2*ZH)/(U(M)**2+KN**2)*JZ11**2
SUMUP=TRMN+SUMUP
1
CONTINUE
C
OUT(M)=CAUS(SUMUP)
CONTINUE
2
C
DO 3 M=2,(NMAX-1)
IF ((OUT(M).LT.OUT(M-1)).AND.(OUT(M).LT.OUT(M+1))) THEN
  BIN=U(M)
ELSE
  ENDF
ENDIF
3
CONTINUE
C
IF (FLAG.EQ.0) THEN
  FLAG=1.
  GO TO 5
ELSE
  PRINT*, 'SCPL BETA = ', BIN
  WRITE(2,*) 'SCPL BETA = ', BIN
ENDIF
STOP
END

```

D. CUT - OFF FREQUENCY

```

* THIS IS THE PROGRAM CALCULATING FOR CUT OFF FREQUENCY OF SCPL
REAL L,LS,LH,D,ER,PI,M,FG,KS,KH,VH,A,TGH,C,F1,F4,F5
COMPLEX VS,THS,F1,F2,CTEMP1,CTEMP2
PRINT*, 'VON BLADEL HIGGINGS CUTOFFS FOR LOADED GUIDE'
C PRINT*, 'ENTER DUTIFILE'
C READ*, FL
OPEN(UNIT=2, FILE = 'FL')
PI = 4*ATAN(1.)
D = .02286
L = .01016
M = 0
C=3F8
* FRACTIONAL HT.. OF DIELEC. LAYER:
LS = 5.77/1000.
* DIEL. LAYER ER:
ER = 10.0
PRINT*, 'GUIDE WIDTH AND HT', D, L
PRINT*, 'DIEL LAYER HT AND ER', LH, ER
LH=-3.37/1000.
PRINT*, 'FREQ. (GHZ) ', 'MAG. (F1) ', 'MAG. (F2) '
WRITE(2,*) 'LS=', LS, 'LH=', LH, 'ER=', ER
DN 99, A=1, 10000
FG= 3.0+.1*A
KS = 20*PI*FG/J
KH= KS*SQRT(ER)
CTEMP1= (KH**2-(M*PI/D)**2*LH )
VH=CSQRT(CTEMP1)
CTEMP2= [ (M*PI/D)**2 - KS**2*LS ]
VS= CSQRT(CTEMP2)
TGH=(CEXP(VH)-CEXP(-VH))/(CEXP(VH)+CEXP(-VH))
TGH = SIN(VH)/COS(VH)
C TGH = C(TGH)
C THS = [ CEXP(VS)-CEXP(-VS) ] / [ CEXP(VS)+CEXP(-VS) ]
F1 = [ VS*THS / (LS*KS**2) ] - [ VH*TGH / (LH*KH**2) ]
F2 = VS / (KS**2*LS*THS) + [ VH*ER / (KH**2*LH*TGH) ]
F3=SQRT(ER)*[2*PI*FG]/C*TAN(SQRT(ER)*2*PI*FG/C)
F4=SQRT(ER)*[2*PI*FG]/C*TAN(2*PI*FG/C)
F5=F3+F4
I=F1*F2
95 FORMAT(IX,3F10.5)
PRINT 55, FG, CAUS(F1), CAUS(F2)
WRITE(2,*) FG, CAUS(F1), CAUS(F2)
WRITE(2,*) 'F5=', F5
99 CONTINUE
END

```

APPENDIX B. IMPEDANCE AND DIELECTRIC CONSTANT BY VARIATIONAL METHOD

A method for computing impedance (Z_0) and effective dielectric constant $\epsilon_{r\text{eff}}$ of the shielded coplanar line (SCPL) is based on the application of the Fourier transform and variational techniques[Ref.10].

The computation was found to be insensitive to the form assumed for the charge distribution on the top ground planes, hence a uniform (negative) charge distribution was assumed.

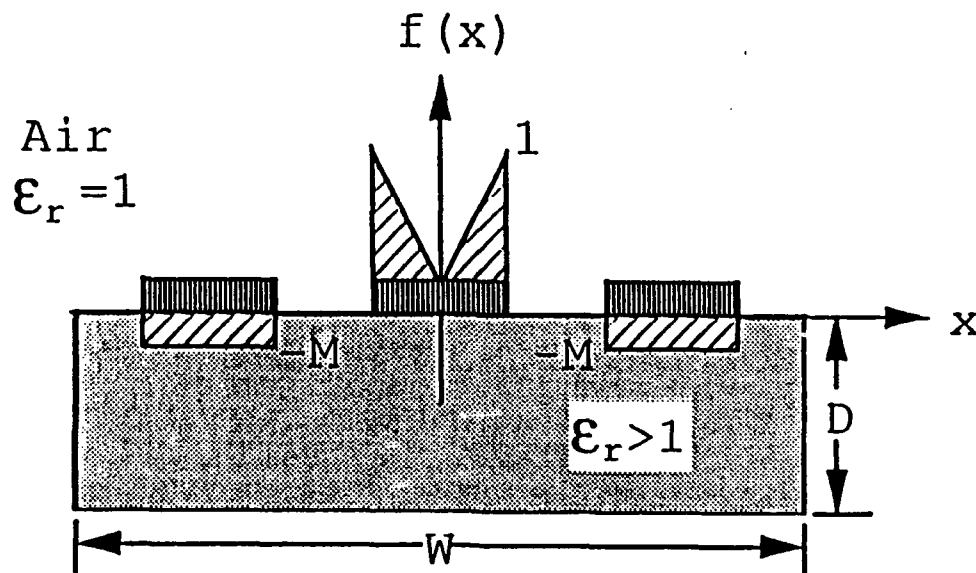


Figure 15. Assumed line-charge density function of SCPL

In case of Fig.15, the assumed elementary charge distribution is:

$$f(x) = \begin{cases} |x| & -\frac{A}{2} \leq x \leq \frac{A}{2} \\ -M & \frac{B}{2} \leq |x| \leq \frac{P}{2} \\ 0 & \text{otherwise} \end{cases} \quad (a1)$$

Where $p =$ the width C in Fig.1.

The Fourier transform of $f(x)$ is :

$$\begin{aligned} \tilde{f}(\beta) = Q & \left[\frac{2\sin(\beta \frac{A}{2})}{\beta \frac{A}{2}} - \left\{ \sin \frac{(\beta \frac{A}{4})}{\beta \frac{A}{4}} \right\}^2 \right. \\ & \left. + \frac{2M}{\beta} \left\{ \sin(\beta \frac{B}{2}) - \sin(\beta \frac{P}{2}) \right\} \right] \end{aligned} \quad (a2)$$

and

$$Q = \frac{A}{2} + M(B - P) \quad (a3)$$

Using the computation given in Ref.10, the characteristic impedance is found to be,

$$Z_o = \frac{1}{v\sqrt{CC_o}} \quad (a4)$$

Where C and C_0 are the variational values of line capacitance with the given dielectric and with air dielectric, respectively.

$$\epsilon_{\text{reff}} = \frac{C}{C_0} \quad (a5)$$

where $v = 3 \times 10^8 \text{ m/s}$, and C_0 is calculated by setting $\epsilon_r = 1$.

LIST OF REFERENCES

1. Tatsuo Itoh, " Analysis of Microstrip Resonators", IEEE Trans. Microwave Theory and Techniques, vol. MTT-22, pp. 946-952 (1974).
2. Tatsuo Itoh, Numerical Techniques for Microwave Passive Structures, John Wiley & Sons., Chapter 5, 1989.
3. Tatsuo Itoh and R.Mittra, "A Technique for Computing Dispersion Characteristics of Shielded Microstrip Lines", IEEE Trans. Microstrip Lines", IEEE Trans. Microwave Theory and Tech. Symposium Digest, pp.693-696 (1987).
4. Y. Shih and T. Itoh, "Analysis of Conductor Backed Coplanar Waveguide", IEEE Trans. Microwave Theory and Techniques, vol.19, pp. 734 (1983).
5. E. Yamashita and R. Mittra, "Variational Method for the Analysis of Microstrip Lines",IEEE Trans. Microwave Theory and Techniques, vol. MTT-16, pp. 251-256 (1986).
6. E. Yamashita," Variational Method for the Analysis of Microstrip Lines", IEEE Trans. Microwave, vol. MTT-16, pp. 529-535 (1968).
7. U. Schulz and R. Pregla, "The Method of Lines for Planar Waveguide, Demonstrated for the Coplanar Line ", Proceedings 10th European Microwave Conference (1980), PP. 331-335.
8. Harry A. Atwater, "Introduction to Microwave Theory", Robert E. Krieger Publishing Co. (1981).
9. Man su. Choi, "Computer Aided Designed Models for Millimeter-Wave Suspended Substrate Microstrip Line", M.S.E.E Thesis, Naval Postgraduate School, CA., March 1990.
10. Jae Soon. Jeong, " An Evaluation of Coplanar Line for Application in Microwave Intergrated Circuitry", M.S.E.E Thesis, Naval Postgraduate School, CA., December 1988.
11. J. Van Bladel and T.J. Higgins, "Cut-off Frequency in Two-Layered Rectangular Wave Guide", Journal of Applied Physics, vol.22, pp.329-333, March 1951.

INITIAL DISTRIBUTION LIST

	No. Copies
1. Defense Technical Information Center Cameron Station Alexandria, VA 22304-6145	2
2. Library, Code 52 Naval Postgraduate School Monterey, CA 93943-5002	2
3. Chairman, Code EC Department of Electrical and Computer Engineering Naval Postgraduate School Monterey, CA 93943 - 5002	1
4. Prof. Harry A. Atwater, Code EC/An Department of Electrical and Computer Engineering Naval Postgraduate School Monterey, CA 93943 - 5002	1
5. Prof. H.M. Lee, Code EC/Lm Department of Electrical and Computer Engineering Naval Postgraduate School Monterey, CA 93943 - 5002	1
6. Library of the Naval Academy Angogok Dong, Chinhae City, Gyungnam 602-00 Republic of Korea	1
7. Hwang, Jung Sub Kyung buk woel sung gun seo meon do gye ri 650 Republic of Korea	3
8. Kim, Chang Ho SMC 1671 N.P.S Monterey, CA 93940.	1

9. Yoon Hee Byung
SMC 2137 N.P.S.
Monterey, CA 93940

1

10. Yi Chong Man
SMC 2917 N.P.S.
Monterey, CA 93940

1